AD_____

Award Number: DAMD17-03-1-0544

TITLE: S14 as a Therapeutic Target in Breast Cancer

PRINCIPAL INVESTIGATOR: William Kinlaw, M.D.

CONTRACTING ORGANIZATION: Dartmouth College
Hanover, NH 03755

REPORT DATE: August 2005

TYPE OF REPORT: Annual

PREPARED FOR: U.S. Army Medical Research and Materiel Command
Fort Detrick, Maryland 21702-5012

DISTRIBUTION STATEMENT: Approved for Public Release;
Distribution Unlimited

The views, opinions and/or findings contained in this report are those of the author(s) and should not be construed as an official Department of the Army position, policy or decision unless so designated by other documentation.

REPORT DOCUMENTATION PAGE

Form Approved
OMB No. 0704-0188

1. REPORT DATE	2. REPORT TYPE	3. DATES COVERED
01-08-2005	Annual	15 Jul 2004 – 14 Jul 2005

4. TITLE AND SUBTITLE

S14 as a Therapeutic Target in Breast Cancer

5a. CONTRACT NUMBER

5b. GRANT NUMBER
DAMD17-03-1-0544

5c. PROGRAM ELEMENT NUMBER

6. AUTHOR(S)

William Kinlaw, M.D.

5d. PROJECT NUMBER

5e. TASK NUMBER

5f. WORK UNIT NUMBER

7. PERFORMING ORGANIZATION NAME(S) AND ADDRESS(ES)

Dartmouth College
Hanover, NH 03755

8. PERFORMING ORGANIZATION REPORT NUMBER

9. SPONSORING / MONITORING AGENCY NAME(S) AND ADDRESS(ES)

U.S. Army Medical Research and Materiel Command
Fort Detrick, Maryland 21702-5012

10. SPONSOR/MONITOR'S ACRONYM(S)

11. SPONSOR/MONITOR'S REPORT NUMBER(S)

12. DISTRIBUTION / AVAILABILITY STATEMENT

Approved for Public Release; Distribution Unlimited

13. SUPPLEMENTARY NOTES

14. ABSTRACT – SEE ATTACHED PAGE

15. SUBJECT TERMS

fatty acids, metabolism, tumor markers

16. SECURITY CLASSIFICATION OF:			17. LIMITATION OF ABSTRACT	18. NUMBER OF PAGES	19a. NAME OF RESPONSIBLE PERSON
a. REPORT	b. ABSTRACT	c. THIS PAGE			19b. TELEPHONE NUMBER *(include area code)*
U	U	U	UU	86	

Abstract

This project aims to determine the importance of "S14", a nuclear protein that signals for lipid synthesis, in breast cancer. Our aims are first, *to develop a model of anti-S14 breast cancer therapy in mice*. Intratumoral adenoviral delivery of an S14-antisense gene into human breast cancer cell xenografts significantly inhibited tumor growth, and we verified the specificity of this effect using siRNA. We identified two siRNAs that knockdown S14 protein in breast cancer cells, and find that they are cytotoxic. Second, *to define the structure of the S14 multimer by X-ray crystallography.* S14 is very difficult to crystallize. We have now used circular dichroism, NMR, and computer modeling to discern the structure of the S14 tetramerization domain. Third, *to define the utility of S14 as a clinical marker*. We produced monoclonal S14 antibodies for an immunohistochemical study of 131 breast cancer cases. This revealed strong associations of S14 staining with invasive tumor size and grade, and a striking power to predict tumor recurrence. Importantly, S14 expression scores did not correlate with those for sex steroid receptors or Her2/neu. Thus, S14 is a *driver* and a *marker* of virulent breast cancer that uniquely identifies cases that are likely to recur.

Table of Contents

Introduction

This project is aimed at defining the potential of protein "S14" as a therapeutic target in breast cancer. S14 is a small, primarily nuclear protein that signals for increased fatty acid synthesis in normal tissues, such as lactating mammary, liver and adipose, in response to fuel-related hormones and nutrients. Most breast cancers have high rates of lipid synthesis, and this promotes their growth and survival. In breast cancer cells, the S14 gene is overexpressed, and this drives their growth. Our aims are to (1) Assess the efficacy of disruption of S14 gene expression in an animal model of breast cancer, (2) Use X-ray crystallographic analysis of purified human S14 to describe the precise geometry of the intermolecular interface in the S14 homotetramer, and (3) Determine S14 expression in an available panel of well-characterized primary human breast cancers, and correlate expression with that of fatty acid synthase (FAS), cyclin D1, and traditional breast tumor markers as well as with disease outcome.

Body

This progress report is organized around the original statement of work, which is reproduced in annotated form below.

Aim #1: Assess the efficacy and toxicity of disruption of S14 gene expression in an animal model of breast cancer.

1) Raise sufficient amounts of recombinant adenoviruses in HEK293 cells, purify and titer the viruses. Months 1-4

This was accomplished.

2) Obtain *nu/nu* mice, establish tumor model in pilot study (estimate 15 mice). Months 4-6

Tumors did not form in our initial pilot studies. Injection of a larger number of MCF7 cells in matrigel solved this problem.

3) Inject mice with breast cancer cells, treat with adenoviruses (estimate 30 mice). Months 6-9

This was accomplished, and data regarding the key variable, tumor growth, are shown in **Fig. 1**. A significant reduction in tumor growth was observed in response to the S14-antisense, as opposed to the control (ß-galactosidase) adenoviral treatment. Due to concerns about the specificity of the antisense effect, we developed a complementary model using a short inhibitory RNA (siRNA). We have tested 6 candidate short inhibitory RNAs (siRNAs) in order to identify a candidate(s) shRNA that could be used either in adenovirus or in a mammary-specific transgene. We used fluorescently-tagged siRNAs to assure adequate transfection efficiency in T47D breast cancer cells.

4) Perform analyses, analyze data. Months 9-12

As shown in **Fig. 2**, two siRNAs caused a substantial knockdown of S14 mRNA and protein in the cells. Importantly, the siRNAs also inhibited the expression of the FAS gene, and caused apoptotic death of the breast cancer cells (**submitted manuscript #1**).

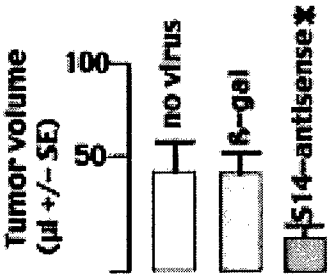

Fig. 1: Effect of adenoviral delivery of S14 antisense mRNA on the growth of MCF7 human breast cancer xenografts in nude mice. Ovariectomized female nude mice with implanted subcutaneous slow-release estrogen pellets (at least 4/group) were injected with 2 x 10^6 MCF7 cells in 50% matrigel into the right and left inguinal mammary fat pads. After 10 d, tumors received 3 sequential treatments, at 6 d intervals, of intratumoral injection of adenovirus harboring either a control gene (ß-gal) or a full-length rat S14 cDNA in the antisense orientation. Tumors were measured with calipers and the volume calculated using a standard formula. Terminal volumes are shown (mean +/- SE, * $p < 0.05$ compared to control or no virus).

Fig. 2: Characterization of effective S14 siRNAs. T47D breast cancer cells were grown to 70% confluence in 6 well plates, and transfected with a scrambled siRNA (negative control) or fluorescently-tagged S14 siRNAs (4 µg/6 well). Transfection efficiency, assessed by FACS, was 86%. Western analysis showed that 2 of 5 candidate siRNAs (siRNA S14-1 and S14-2) abrogated S14 protein expression. (siRNA#1 shown in **panel A**), and S14 mRNA levels were also reduced **(panel B)**. Expression of FAS mRNA was inhibited by the S14 knockdown **(panel C)**, as previously observed in hepatocytes treated with S14 antisense. Assessment of cell viability using the MTS assay showed a major cell dropout by 3 d post-transfection **(panel D)**. Ad-S14-antisense produced the same effects as siRNA. Disturbed cellular architecture, nuclear disorganization, and DNA fragmentation typical of apoptosis were evident on phase contrast and fluorescent microscopy of Hoechst-stained cells, and the TUNEL assay by 3 d postinfection, while the control (Ad-ß-gal) was without effect **(panel E)**. Importantly, S14 siRNAs and Ad-S14-AS had no effect on the growth of nontumorigenic, MCF10a mammary epithelial cells, which express very low levels of S14.

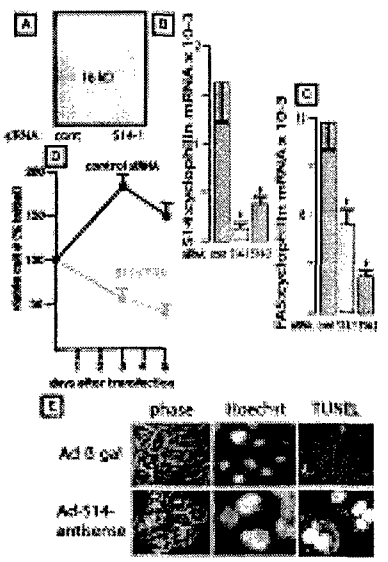

Aim #2: Use X-ray crystallographic analysis of purified human S14 to describe the precise geometry of the intermolecular interface in the S14 homotetramer.

1) Subclone the human S14 cDNA into the pROEX-HT vector, express and purify protein. Months 1-6

This was accomplished. The sequenced cDNA was subcloned, expressed in bacteria as a 6 x HIS fusion, and purified on Ni-agaraose, followed by cleavage of the tag with TEV protease and removal of the protease and cleaved tag to yield pure human S14. This material was also used as an immunogen in mice to elicit monoclonal antibodies used for for Aim 3.

2) Assess crystallization conditions, optimize. Months 6-10

This continues to be difficult. Purified protein produced in our laboratory was used in crystallization screens in Dr. Amy Anderson's laboratory. Analysis using a panel of "standard" crystallization conditions showed the protein to be coagulated rather than crystallized. Dr. Anderson has subsequently used > 500 different sets of conditions, to no avail. We have analyzed the bacterially-expressed protein on denaturing and nondenaturing gels, in an attempt to visualize interfering contaminants (N-terminal truncated S14 fragments were seen), and to

assess the folding and multimerization of the protein under nondenaturing conditions. This revealed that 1) the protein does form multimers consistent with a tetramer, and 2) that there are two forms of the monomer that appear to be folding variants, the "proper" one being the least abundant.

With the guidance of Dr. Anderson we undertook alternate approaches, including:

- Circular dichroism analysis of a peptide representing the proposed C-terminal interaction domain of S14 showed that the region is alpha-helical in solution (**Fig. 3** shows classical peak at 190, and nadir at 210 nM), as was predicted by computer modeling. Thus, the structure of that region is typical of an interaction domain.
- NMR analysis of the interaction domain in solution verified the alpha-helical configuration, revealed that S14 forms homotetramers, and showed that the alpha-helices are bundled in parallel.
- Computer modeling of the carboxyl-terminal multimerization domain, guided by the aforementioned observations, predicted a key role for tyrosine 138 and lysine 127 in the interaction. We mutated Tyr138 to alanine, and expressed the protein in bacteria, followed by western analysis. This indicated that the mutation had a profound effect on the physical chemistry of S14, as it rendered the protein totally insoluble in the bacterial pellet (**Fig. 4**).

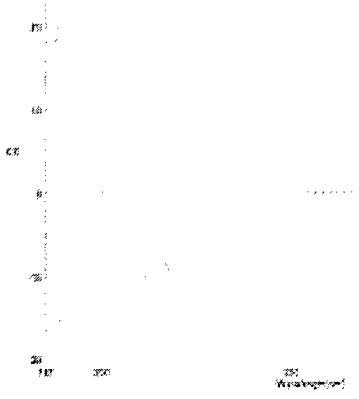

Fig. 3: Circular dichroism analysis of the S14 domain.

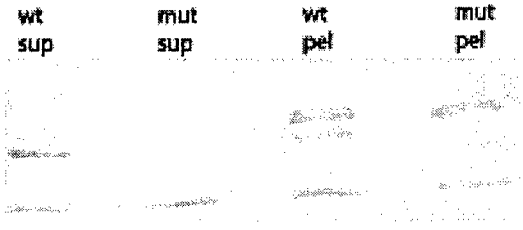

Fig. 4: Effect of Y138A mutation on the production of soluble S14 in bacteria. Western blot of S14 in soluble supernatants sup) and insoluble pellet (pel) from IPTG-induced wild type (wt) and mutant (mut) S14 pro-ducing cells is shown. Purple bands at the bottom of lanes are the dye front (Pyronin Y).

Summary- Our data demonstrate the C-terminal S14 self-interaction domain to be helical in solution, where it forms a tetramer in parallel orientation. Moreover, Y138 may be a vulnerable point for assembly of soluble tetrameric S14. Of note, Y138 is conserved in all S14 and S14-related peptide homologs from zebrafish to humans.

3) Obtain X-ray crystallographic structure. Months 10-24

This will require tandem affinity purification of the protein from bacterial lysates, and isolation of the properly-folded species.

4) Validate critical residues in *in vivo* systems (yeast two-hybrid, co-immunoprecipitation), define effects of candidate dominant negative mutations in breast cancer cells. Months 15-36

This has been done for Y138; further progress awaits crystallization.

5) Model drug candidates based on the above information, test in cell culture and mouse model system. Possibly Months 30-36, and beyond

Aim #3: Determine S14 expression in an available panel of well-characterized primary human breast cancers, and correlate expression with that of FAS, cyclin D1, and traditional prognostic factors as well as disease outcome.

1) Optimize nonstandard immunohistochemical techniques (ie- those not in general clinical use, including S14, and FAS). Months 6-12

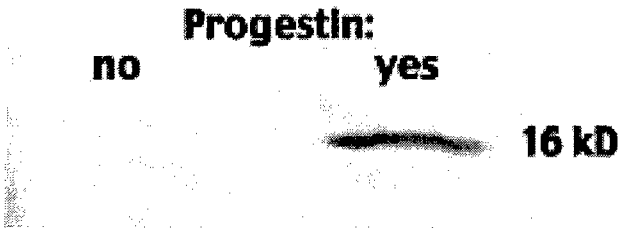

Fig. 5: Detection of S14 protein in T47D breast cancer cells by western blot using monoclonal anti-S14 antibody "#2". Cells grown in charcoal-stripped fetal calf serum were treated with progestin (10 nM R1881) or vehicle for 48 h. Cellular extracts (100 μg protein/lane) were analyzed using crude hybridoma supernatant at 1:1000 dilution.

This has been accomplished. The major issue was nonspecific staining seen with our previous polyclonal anti-peptide human S14 antibody preparation. We worked with Dr. Peter Morganelli, Norris Cotton Cancer Center (Dartmouth Medical School), to develop highly specific monoclonal antibodies. Antibody development was funded by another source. We used tbacterially-expressed human S14 as an immunogen in mice, and also used it to screen for positive clones by ELISA. We identified two antibodies that show single bands of the appropriate size on western analysis of human breast cancer cells (results for antibody "#2" shown in **Fig 5**), and yield excellent results in immunohistochemistry of human breast cancer sections (representative result shown for antibody #2 in **Fig. 6**).

2) Cut blocks, perform immunohistochemistry. Months 12-18

This is completed for S14, cyclin D1 and FAS on 131 breast cancer blocks, and twenty samples of normal mammary tissue obtained at reduction mammoplasty.

3) Score samples for marker expression. Months 18-24

This has been completed and validated by Dr. Wells.

4) Collate clinical variables. Months 1-24

Data regarding clinical course, histological stage and grade, response to therapy, and expression of standard clinical markers and cyclin D1 were collated by Dr. Schwartz.

5) Perform statistical analyses. Months 24-30

Statistical analyses have been performed by Dr. Cole, and his assistant, Jennifer Chambers. These studies have yielded striking results, summarized below.

Patients- We studied 131 breast cancer cases consecutively diagnosed at Dartmouth in 1997-98; 44 ductal carcinomas in situ (DCIS), 34 node (-) breast cancers, and 54 node (+) breast cancers, and 20 samples from women without breast cancer (10 pre-, 10 post-menopausal). Cases are characterized for ER, PR, Her2/neu, tumor stage, grade, and size, patient demographics, and disease-free survival over 3000 days. S14 and FAS

immunohistochemistry are shown in **Fig. 6** (antibody characterization for this application and details of the criteria used for scoring S14 and FAS are detailed in **manuscript #2**).

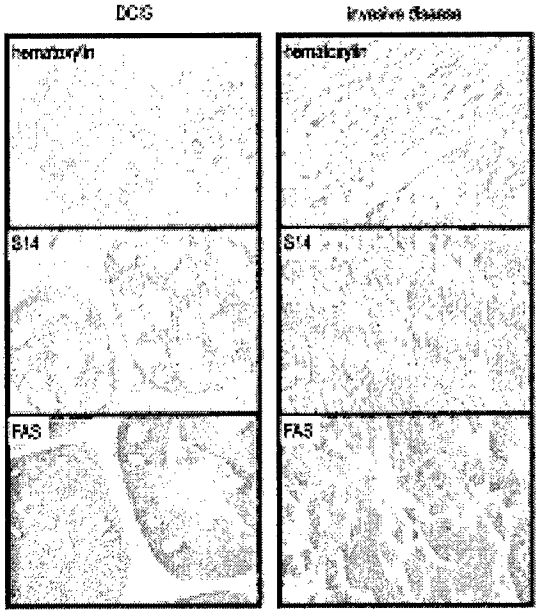

Fig. 6: Examples of DCIS (left) and invasive breast cancer (right) demonstrating high immunohistochemical scores for S14 and FAS. Slides are counterstained with hematoxylin. The S14 signal is primarily nuclear, FAS is cytoplasmic. Tumors were scored by collaborator Dr. Wendy Wells (Pathology Department, Dartmouth Medical School), without access to clinical data, and were independently verified by scoring of 20 randomly chosen slides for each antibody by another pathologist, with 100% concordance. Scores were 0 (no staining), 1+ (faint signal), or 2+ (strong stain, as in examples shown).

Intensity of S14 expression increases with histological indices of tumor aggressiveness- S14 was observed in normal mammary epithelial cells, whether from women with no history of breast cancer (reduction mammoplasty samples, n=20) of both pre- and postmenopausal status, or in normal tissue adjacent to tumors. In tumors, however, the frequency of 2+ scores rose sharply with tumor grade. In DCIS strong staining increased to 97% in grade 3 cases ($p=0.003$). Likewise, all grade 3 invasive tumors (node - and +) exhibited a 2+ score ($p<0.001$). S14 expression also increased with tumor size ($p=0.05$). S14 scores did not vary with tumor stage, indicating that activation of the S14 gene occurs early in tumorigenesis, rather than being acquired during tumor progression. The statistical methods we used are detailed in submitted **manuscript #2**.

FAS staining- In DCIS, the relationship between FAS expression and tumor grade nearly reached significance ($p=0.08$), as reported [36], but no relationship was seen in invasive cases, as nearly all showed maximal expression.

Comparison with tumor markers and cyclin D1- There was no correlation of S14 scores and ER, PR, or Her2/neu expression. In both DCIS and invasive cases there was no relationship between S14 and cyclin D1 levels. Cyclin D1 did not predict reduced survival, but Her2/Neu did ($p=0.05$).

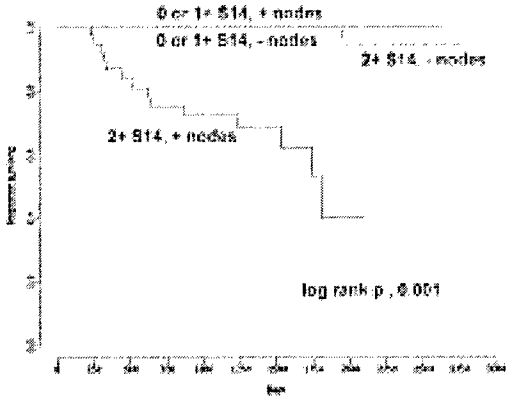

Fig. 7: Disease free survival (Kaplan-Meier) in 88 patients with invasive breast cancer segregated by S14 score and nodal metastasis. No tumors with 0 or 1+ S14 scores recurred, whether lymph nodes were involved (n=10) or not (n=11)(upper tracings, superimposed). One patient of 23 with 2+ S14 and negative nodes recurred at ~2000 d. All other recurrences were in the 2+ S14, positive nodal metastasis group (14 of 44 recurred; lower tracing). Log rank $p<0.0001$.

S14 staining intensity predicts patient outcome- For all invasive tumors there was a relationship ($p=0.015$) between the level of S14 and disease-free survival over 3000 days. Indeed, none of the 21 cases exhibiting a

score of 0 or 1+ recurred, whereas 32% of the 67 cases with 2+ S14 scores did. Importantly, we observed separable effects of S14 and the presence of nodal metastases on disease-free survival in invasive disease **(Fig.7)**. Among 34 node (-) cases, only one recurrence was seen, and it exhibited a 2+ S14 score. Strikingly, among 10 node (+) cases with weak S14 expression, there was no recurrence. In contrast, of the 44 node (+) cases with strong staining, 14 (32%) recurred (log rank $p<0.0001$).

Summary- S14 specifies a subset of patients that differ from those selected by conventional breast cancer markers or cyclin D1. Thus, despite coamplification of S14 and cyclin D1, we do not find a functional interaction between these nuclear proteins. We also observed no correlation of S14 and sex steroid receptor expression, despite S14 induction by progestin in T47D cells. Tumors with high S14 scores have higher grade, are bulkier, and are likely to recur. Conversely, no case with low S14 recurred, irrespective of lymph node metastasis. Taken alone, this study identifies S14 as a *marker* of virulent breast cancer. In concert with our data from breast cancer cells, S14 is also identified as a *driver* of aggressive breast tumor biology. This work was presented at the Era of Hope Breast Cancer Meeting in Philadelphia in June, 2005, and is submitted for publication **(Appendix manuscript #2)**.

Key Research Accomplishments

1) Preliminary demonstration of efficacy of anti-S14 gene therapy in an animal model.
2) Confirmation of the above in tissue culture using siRNA.
3) Expression of human S14 protein in bacteria.
4) Direct proof of the alpha-helical configuration of the S14 mulitmerization domain, demonstration that it forms homotetramers in solution in parallel bundles, and identification of tyrosine 138 as critical for the assembly of soluble S14.
5) Characterization of anti-S14 monoclonal antibodies useful in Western and immunohistochemical analyses.
6) Demonstration of brisk expression of S14 in the earliest stage of breast cancer (DCIS), to a level equal to that seen in lactating mammary epithelium.
7) Elucidation of tight correlations of S14 the level of S14 expression with breast tumor size and histological grade, and a striking predictive value for disease-free survival in invasive breast cancer.
8) Demonstration that S14 identifies a unique subset of aggressive breast cancer cases that differs from those identified by traditional markers and cyclin D1.

Kinlaw, William B. Appendix item #1

S14 protein in breast cancer cells: direct evidence of regulation by SREBP-1c, superinduction with progestin, and effects on cell growth.

Peter M. Martel[1,3], Chad M. Bingham[1,3], Charles J. McGraw[1,3], Christina L. Baker[1,3], Peter M. Morganelli[2,3], Marie Louise Meng [1,3], Jessica M. Armstrong [3,4], Joel T. Moncur [1,5], and William B. Kinlaw[1,3]

Department of Medicine, Division of Endocrinology[1], Department of Microbiology and Immunology[2], the Norris Cotton Cancer Center[3], and the Department of Physiology[4], Dartmouth Medical School; current address Walter Reed U. S. Army Medical Center [5]

Correspondence may be addressed to:
William Kinlaw, MD
Department of Medicine and The Norris Cotton Cancer Center
Dartmouth Medical School
606 Rubin Building
1 Medical Center Drive
Lebanon, NH 03756

Tel- 603-653-9961
FAX- 603-653-9952
E-mail: william.kinlaw@hitchcock.org

Keywords: spot 14, THRSP, SREBP1, spot 14 related peptide, CHREBP, fatty acid synthase, progesterone, T47D cells

Running title: Spot 14 in breast cancer cells

Abstract

Most breast cancers express high levels of the enzymes of fatty acid synthesis, and require lipogenesis for survival. We previously demonstrated that Spot 14 (S14), a nuclear protein that activates lipogenesis-related genes in hepatocytes, is overexpressed in lipogenic breast cancers, but the cause of the overexpression was not known. Sterol response element-binding protein-1c (SREBP-1c) is a transcription factor required for induction, by insulin, of lipogenesis-related genes including S14 and fatty acid synthase (FAS) in hepatocytes. Studies correlating SREBP-1c and FAS expression in several types of cancer suggested that SREBP-1c may also drive breast cancer lipogenesis. We directly examined the hypothesis that SREBP-1c drives the expression of S14, and mediates lipogenic effects of progestin (PN) in T47 D breast cancer cells. PN induced S14, FAS, and SREBP1c mRNAs. A dominant-negative SREBP-1c mutant inhibited the induction of S14 and FAS mRNAs by PN. Conversely, an active SREBP-1c mutant induced S14 and FAS mRNAs in the absence of hormone, and superinduced in its presence. Changes in S14 mRNA were reflected at the protein level. The proximal 4003 bp of the S14- and 157 bp of the FAS gene promoters were sufficient to mediate PN-induced transcription. Knockdown of S14 mRNA and protein using siRNA or antisense RNA reduced, whereas overexpression stimulated, T47D cell growth. Nontumorigenic MCF10a mammary epithelial cells express low levels of S14, and were not growth-inhibited by S14 siRNA. These data directly demonstrate that SREBP-1c drives S14 gene expression in breast cancer cells, and that progestin magnifies that effect, possibly via the action of carbohydrate response element-binding protein. Our results support the prediction that S14 augments breast cancer cell growth and survival, based on S14 gene amplification and protein overexpression observed in actual breast tumors.

Introduction

S14 is a primarily nuclear protein that is abundant in tissues active in long chain fatty acid synthesis, including lactating mammary gland (reviewed in [1]). We previously demonstrated that the S14 gene on chromosome 11q13 may be amplified in breast cancer cells, and that S14 protein is overexpressed in most breast cancers [2]. Concordant overexpression of S14 and acteyl CoA-carboxylase, the rate-determining enzyme of long chain fatty acid synthesis, indicated that S14 is a component of the lipogenic phenotype observed in a subset of aggressive breast cancers. Taken together, the observations of gene amplification, frequent S14 protein overexpression, and association with enhanced lipid metabolism suggested that S14 could influence the growth of breast cancers. This prediction was strongly supported by our recent analysis of S14 expression in 131 breast cancer cases, which demonstrated striking associations of S14 overexpression with high-grade and bulky tumors, and with reduced disease-free survival [3].

The lipogenic tumor phenotype is characterized by high rates of fatty acid synthesis, elevated tumor content of lipogenic enzymes such as fatty acid synthase (FAS), and dependence on lipogenesis for tumor cell growth (reviewed in [4]). The latter was shown by Pizer and coworkers using cerulinen, a pharmacological inhibitor of fatty acid synthase that caused apoptosis of breast cancer cells [5], and inhibited the growth of human ovarian tumor cell xenografts in nude mice [6]. Likewise, the anti-obesity drug Orlistat, also a FAS inhibitor, caused apoptosis of lipogenic prostate cancer cells in culture and in xenografts in immunodeficient mice [7].

In hepatocytes, S14 and lipogenic enzymes are inducible by insulin, glucose metabolism, and thyroid hormone (reviewed in [1]). The lipogenic effects of insulin are substantially mediated at the gene level by sterol response element-binding protein 1c (SREBP-1c), a transcription factor that resides in the endoplasmic reticulum until insulin activates its translocation to the Golgi, where the active fragment is released by proteolysis, permitting transit to the nucleus to activate gene transcription ([8], reviewed in [9]). It is attractive to hypothesize that in breast cancer cells, as in the liver, SREBP-1c is the major driver of lipogenic gene expression. To date, this issue has been addressed in studies of breast cancer specimens [10], colon cancer specimens and cells [11], and prostate cancer cells [12-14]. The studies of breast and colon cancer correlated expression of FAS and SREBP-1c, but did not include mechanistic experiments. In contrast, the studies in prostate cancer cells did demonstrate a dependence of androgen- and growth factor-induced expression of FAS on SREBP-1c. Moreover, processing of the extranuclear SREBP-1c precursor was increased by androgen induction of SREBP cleavage-activating protein (SCAP), the protein responsible for escorting SREBP-1c to the Golgi, where proteolytic activation occurs. In contrast to the enhancement of SREBP-1c processing by androgen in prostate cancer cells, however, Heemers and coworkers saw no increase in nuclear SREBP-1c content in progestin-treated T47D cells demonstrating S14 gene induction [15].

We have now focused on the regulation of S14 mRNA and protein expression by progestin in breast cancer cells, and the role of SREBP-1c in the action of the hormone. Our results provide mechanistic evidence that induction of S14 mRNA and protein by progestin in breast cancer cells requires the action of SREBP-1c. Several lines of evidence, however, suggested that this action

of progestin is not mediated directly. We further provide evidence for a role of S14 in the growth and survival of breast cancer cells.

Materials and Methods

Recombinant adenovirus- Adenovirus harboring dominant-negative and constitutively active SREBP-1c mutants were kindly supplied by F. Foufelle (Paris, France [16]). A full-length rat S14 cDNA ([17]; sense orientation, Ad-S14; antisense orientation Ad-S14-AS) or ß-galactosidase gene (negative control; Ad-ß-gal) were inserted into adenoviral DNA (Clontech) essentially as described in [18]. Adenovirus for expression of a dominant-negative Max-like factor x (Mlx) was kindly supplied by H. Towle (U. MN). Viruses were propagated in HEK293 cells (ATCC) and titered by immunocytochemical analysis for a capsid protein (Rapid-Titer, Clontech). The multiplicity of infection (MOI) required for quantitative infection was determined by staining Ad-ß-gal-infected wells.

Cell culture and infection- T47D cells (ATCC) were grown in RPMI 1640 plus 10 µg/ml insulin, HEK293 cells (ATCC) in RPMI 1640, and MCF10a cells in DMEM/F12 plus 4 mg/ml insulin, 20 g/ml epidermal growth factor, and 1 mg/ml hydrocortisone. Media contained penicillin, streptomycin, 4 mM glutamine, and 10% fetal calf serum unless noted. Charcoal-stripped fetal calf serum (Hyclone) was used in studies involving R5020 or R1881 (10 nM, New England Nuclear): an equal volume of ethanol vehicle was added to control cultures. Cerulinen (Sigma) was used at 10 µg/ml.

Plasmid transfection- T47D or HEK 293 cells were plated at 50% confluence in 75 cm^2 flasks and the next morning were transfected with 8 µg plasmid DNA in 48 µl Fugene (Roche) in 5%

charcoal-stripped serum-containing media without antibiotics. In order to ensure uniform transfection efficiency, cells were trypsinized, mixed, and redistributed into 6 well plates 8 h later: 48 h post-transfection, culture medium was removed, and extracts prepared in reporter lysis buffer (Promega, 250 µl/well. Lysates (20 µl) were assessed for luciferase activity using a LMaxII384 luminometer (Molecular Devices), and normalized to protein concentrations (BCA Protein Assay, Pierce).

Transfection of siRNA- Cells were plated at ~70% confluency in 60mm dishes the day before transfection with 20µg siRNA in 333µl diluent supplied by Qiagen, and 120µl of RNAifect Transfection Reagent (Qiagen). The siRNAs (Dharmacon) targeted the following sequences in S14 mRNA: siRNA#1- 5'-ggaaatgacgggacaagtt-3'; siRNA#2- 5'-cagccgaggtgcacaacat-3'. Complexes were incubated at room temperature for 15 min and added drop-wise to cultures. After 24 h cells were trypsinized and redistributed into 4 wells of a 12 well plate to ensure uniform transfection efficiency, in media containing hormone or vehicle.

Preparation of anti-S14 antibody and western blot- Monoclonal antibody against human S14 was prepared in the Norris Cotton Cancer Center antibody resource (Dartmouth Medical School) using a protocol approved by the Institutional Animal Care and Use Committee. Hybridomas were prepared from splenocytes of mice immunized with glutathione-S-transferase (GST)-tagged human S14 expressed from vector pGEX-3X (Amersham) in *E. coli*. Female Balb C mice were immunized intraperitoneally with 50 µg GST-S14 mixed in RIBI adjuvant (Sigma), and boosted with 20 µg antigen in adjuvant 3 and 6 weeks later. Splenocytes were fused with NS1 cells

(ATCC) 4 d later. Screening was by ELISA using wells coated with His_6-tagged S14 expressed in bacteria from vector pROEx-HT (Life Technologies). Crude supernatant (1:1000 dilution of hybridoma "KVB7", an IG2a) or anti-HA (Sigma) were used in western analysis with protein A-alkaline phosphatase conjugate for detection of S14 or HA-tagged S14-related peptide, respectively, as described [17].

Reverse transcriptase-PCR- Total RNA (500 ng) harvested in Trizol was used as template with the GIBCO/BRL "OneStep" kit. Primers (forward/reverse) for S14 were 5'-ccatctgtgtggatgtggacc-3'/5'-agcatcccggagaactgagcc-3', SREBP-1a 5'-tcagcgaggcggctttggagcag-3'/5'-catgtcttcgatgtcggtcag-3' [19]; SREBP-1c: 5'-ggaggggtagggccaacggcct-3'/5'-catgtcttcgaaagtgcaatcc-3' [19], FAS: 5'-acagggacaacctggagttct-3'/5'-ctgtggtcccacttgatgagt-3' [20]. S14-RP was analyzed with two sets of primers, one that amplified the entire coding region: 5'-acccggccgaccatccc-3'/5'-agtttgcagtctgcccttccc-3', and a nested pair: 5'-ccgggttagacaacgatgtt-3'/5'-tggctgtacatgtcccgagag-3'. PGC-1ß primers were: 5'-acctcacctcggcacagtgct-3'/5'-tcacccggctccttgtcct-3', and those for CHREBP were 5'-ccgcctgaggatgcctacgtc-3'/5'-ggaggcgggagttggtaaaga-3'. Sizes of the products (bp) were: S14 365; SREBP-1a 80; SREBP-1c 80; FAS 159; S14-RP 724 and 132; PGC-1ß 99, and CHREBP 116. Amplification was at 55° x 30 min, 94° for 2 min, followed by 15 cycles each of 94° x 30 seconds, 57° x 30 seconds, 72° x 1 min; 94° x 30 seconds, 62° x 30 seconds, 72° x 1 min; 94° x 30 seconds, 55° x 30 seconds, 72° x 1 min, followed by extension at 72° x 2 minutes. Reactions using primers that did not span introns were always accompanied by a control PCR devoid of reverse transcriptase, which never yielded a product.

Real time reverse transcriptase PCR- Total RNA was isolated using RNeasy minicolumns from cell extracts prepared with QiaShredder (Qiagen,). RNA integrity was assessed by visualization on agarose gels, and contamination with genomic DNA was excluded by failure to obtain a PCR product using primers for cyclophilin A. RNA (1μg) was reverse-transcribed with M-MuLV reverse transcriptase and $p(dt)_{18}$ (New England Biolabs). Product (50 ng) was added to 96 well plates (in duplicate) with primers and SYBR Green reaction mix (PE Biosystems). PCR (Bio-Rad MyIQ Icycler) commenced with heat activation for AmpliTaq Gold DNA polymerase (Roche) (95 °C for 10 min), followed by denaturation (95° for 30s), annealing (57°, 30 s), extension (72°, 30 s), and data acquisition at the end of the extension step, for 40 cycles. Dilutions of cloned cDNA fragments from each mRNA assayed were included to provide a standard curve. MyIQ Optical System Software (Bio-Rad) was used to assess signals during the log-linear accumulation phase, calculated as ng template per tube compared to the standard curve, which was linear across 6 logs of input. Values were normalized to the signal obtained from the same sample using primers for cyclophilin A and reported in arbitrary units. Melting curves assured that signals arose from single products, and wells without template were included to survey for contamination.

Cell growth- Cells (20,000/well) were seeded in 12 well plates in media containing stripped fetal calf serum. Medium was replaced after 12 h, and 12 h later with media containing 10 nM R1881 (or R5020) or vehicle. Media were replaced again after 3 d, and growth was assayed on the 6th day after hormone addition. In experiments using adenovirus, cells (20,000/well) seeded in medium containing 10% fetal calf serum were infected the following morning. Media were changed after 1 h, and again 3 d later. Cell accumulation was measured by the 3-(4,5-

dimethylthiazol-2yl)-5-(3-carboxymethyphenyl)-2-(4-sulfophenyl)-2H-tetrazolium (MTS) assay (Promega). Oxidation of MTS by viable mitochondria yields a product that absorbs at 490 nM. MTS data showed a strong correlation with DNA content/well under a variety of metabolic circumstances (not shown).

Results

SREBP-1 gene expression in T47D cells- RT-PCR analysis of hepatoma (HepG2, known to express both SREBP-1 isoforms [19]), lipogenic breast cancer (T47D [21]), and non-lipogenic cervical adenocarcinoma (HeLa [22]) cells showed that both SREBP-1 isoforms are expressed in these cell types (**Fig. 1**).

Effect of progestin on lipogenesis-related mRNAs- Real time RT-PCR, using cyclophilin as a control, showed that S14, FAS, and SREBP-1c mRNAs were significantly induced by 10 nM R1881 within 48 h (**Fig. 2, panel A**). A timecourse using 10 nM R5020 showed induction of S14 and FAS mRNAs comparable to that observed with R1881 (**panel B**). There was a lag time of > 10 h between application of the hormone and the onset of accumulation of S14 and FAS mRNAs.

Progestin induces S14 and FAS gene transcription- We used a human S14 gene promoter fragment fused to a luciferase reporter to determine the mechanism underlying R1881-induced accumulation of S14 mRNA (**Fig. 3 A**). The human S14 construct (kindly supplied by C.

Mariash, U. Minnesota) contained the proximal 4003 bp of the promoter [23]. This fragment does not contain a canonical progesterone response element [24]. Nevertheless, R1881 induced promoter activity by 4-fold. We employed a 157 bp fragment of the human FAS gene promoter that is also devoid of progesterone response elements to examine the effect of R1881 on that gene (**Fig. 3 B**; kindly supplied by J. Swinnen, Leuven, Belgium [12]). A 4-fold induction was observed after 48 h exposure to the hormone (left), and the response from a construct with the sterol response element deleted was markedly reduced (right).

Effects of SREBP-1c on S14 mRNA and protein induction by progestin- We delivered SREBP-1c mutants *via* adenoviral vectors to assess the role of SREBP-1c in S14 gene activation by progestin. Cells were grown in charcoal-stripped fetal calf serum for 48 h and then infected with adenoviruses (MOI 50) for 1 h in the same medium. R1881 (10 nM) or vehicle were added after 8 h, and RNA was harvested 40 h later. S14 mRNA was induced ~ 8-fold in the presence of the control adenovirus (Ad-ß-gal) (**Fig. 4, panel A**). Basal S14 expression was unaffected by the dominant negative mutant (Ad-SREBP-1c-DN), while induction was reduced to 2.5-fold. Constitutively active SREBP-1c (Ad-SREBP1c) in the absence of R1881 caused a major induction of S14 mRNA, 330-fold over the basal value seen in the presence of Ad-ß-gal without R1881, while Ad-SREBP plus R1881 superinduced, to ~1300-fold above the unstimulated level.

Western analysis using a S14 monoclonal antibody showed effects on S14 protein concordant with those of the mRNA (**Fig. 4, panel B**). Cells were grown in media containing stripped fetal calf serum for 48 h, and then, with or without preceding adenoviral delivery of the constitutively

active SREBP-1c mutant, exposed or not to 10 nM R1881 for 48 h. No S14 was appreciable in cells cultured without hormone or Ad-SREBP-1c. A faint band of the appropriate size (~ 16 kD) was seen after stimulation with R1881 alone, while a strong signal appeared after exposure to Ad-SREBP-1c. As was the case for S14 mRNA, application of both stimuli induced S14 protein above the level seen with SREBP-1c alone.

S14-related peptide- S14-RP is ancestral to the S14 gene, its predicted molecular weight is 20,201 D, and it shares strong homology to three domains of S14 (amino terminal and mid-molecule hydrophobic domains, and an alpha-helical carboxyl-terminal zipper domain [25]). The tissue distribution of S14-RP differs from that of S14 in rodents [26]. RT-PCR using two different primer pairs indicated that S14-RP transcripts occur in T47D cells (**Fig. 5, panel A**). We used real time-RT-PCR to determine whether the S14-RP gene was responsive to progestin, and found no significant difference in R5020-treated T47D cells 48 h after hormone addition (**Fig. 5, panel B**). It was important to determine whether the S14 antibody recognized S14-RP. We expressed a full length human S14-RP cDNA (OpenBiosystems) with a hemagglutinen (HA) tag appended to the amino terminus from vector pCGN (kindly supplied by Dr. Lynn Sheldon, Dartmouth Medical School) transiently transfected it into HEK293 cells, and performed western analysis with anti-hS14 monoclonal or anti-HA antibodies (**Fig. 5, panel B**). The anti-HA blot demonstrated a band of appropriate migration (~ 20 kD). No signal, however, was observed on the blot probed with the anti-hS14 antibody. This finding, the concordant regulation of S14 mRNA and protein described above, and the disappearance of the band upon treatment with S14-specific small inhibitory RNA (see below), indicated that the antibody is specific for S14.

Given the evolutionary conservation of the putative interaction domains of S14 and S14-RP [25], we performed experiments to determine whether the two peptides can form heteromeric complexes (data not shown). We used the same approach that demonstrated multimerization of S14 [27]: cotransfection of GST-S14 and HA-S14-RP expression plasmids was followed by absorption of cell lysates on glutathione agarose and western analysis of bound proteins on duplicate blots for S14 and HA. Each of the peptides was expressed, but HA-S14-RP was not released from the beads, indicating that the two peptides to not physically interact (data not shown).

Effects of SREBP-1c on FAS mRNA and induction by progestin- We analyzed the experiments shown in Fig. 4 to determine if FAS gene expression was also superinduced by combined SREBP-1c and progestin stimulation. FAS mRNA was induced ~2-fold by R1881 in the presence of Ad-ß-gal (**Fig. 6**). Basal FAS mRNA expression was slightly reduced by Ad-SREBP-1c-DN, while hormonal induction was abrogated. Ad-SREBP1c in the absence of R1881 induced FAS mRNA content to a level comparable to that seen after infection with Ad-ß-gal in the presence of hormone, and Ad-SREBP plus R1881 further increased FAS mRNA accumulation.

Do T47D cells express the peroxisome proliferator activated receptor-gamma coactivator-ß (PGC-1ß) and/or carbohydrate response element binding protein (CHREBP) genes? PCG-1ß and CHREBP are factors that may facilitate the action of SREBP-1c. We assessed the possibility

that these candidate mediators of the superinduction of S14 gene expression by SREBP-1c and progestin were expressed in T47D cells using RT-PCR. We found no evidence of PGC-1ß gene expression (**Fig. 7 panel A**). In the case of CHREBP, however, a band of the expected size was amplified from T47D cell template (**panel B**, rightmost lane). We further analyzed a panel of cell lines, including those representing lipogenic mammary cancer (MCF7, SKBR3, ZR75.1, T47D), nonlipogenic breast cancer (MDA-MB-435s), nontumorigenic mammary epithelium (MCF10a), embyonic kidney (HEK293), hepatocarcinoma (HepG2), and nonlipogenic cervical adenocarcinoma (HeLa). A signal was consistently generated from each cell line except MCF10a and MDA-MB-435s.

Using real time RT-PCR, we found that, in contrast to SREBP-1 mRNA, CHREBP mRNA was not induced by progestin (not shown). We assessed a panel of five siRNAs for inhibition of CHREBP expression, as has been reported in hepatocytes [28], and none were effective in reducing levels of CHREBP mRNA. Mlx is the obligate heterodimerization partner of CHREBP [29], and a dominant negative Mlx mutant blocks the activation of glucose-responsive genes in hepatocytes [30]. We infected T47D cells with adenovirus harboring a dominant negative Mlx mutant (MOI 50, kindly supplied by H. Towle, U. MN), and observed gross distortion of cellular architecture and cellular dropout within 4 d of infection (**panel C**).

Do levels of S14 affect T47D cell growth? Enforced overexpression was achieved by infecting cells with adenovirus harboring a full length rat S14 cDNA (**Fig. 8**). Western analysis of cell lysates collected 3 d after adenoviral infection using an antibody specific for rat S14 revealed no signal from cells infected with control adenovirus (Ad-ß-gal) (**panel A, lane 2**), or an adenovirus

harboring the S14 cDNA in the antisense orientation (**lane 3**). Infection with Ad-rS14, however, yielded a strong band of the appropriate size (~17 kD, **lane 4**), of intensity comparable to that observed in liver from a hyperthyroid rat fed a fat-free, high carbohydrate diet (**lane 1**). Infection with Ad-rS14 accelerated the accumulation of the cells by 45% above that observed after infection with Ad-ß-gal after 5 days (**panel B**). Similar effects were observed in MCF7 and SKBR3 breast cancer, but not HepG2 hepatocarcinoma cells (not shown).

We attempted to reduce S14 mRNA and protein expression using short inhibitory RNA (siRNA). We found that T47D cells were difficult to transfect with siRNA, owing to variable transfection efficiency between experiments. The cause of the variability was not clear, except that highly passaged cells appeared less susceptible to transfection (data not shown). Using low passage number cells (< 8), we transfected fluorescent-tagged siRNA (fl-siRNA) in each experiment, followed by FACS analysis 4 h later to monitor transfection efficiency (**Fig. 9, panel A**). Only experiments with transfection efficiency > 80% were analyzed further. We scrutinized the cells by laser confocal microscopy 4 h after transfection of fl-siRNA to assure that the siRNA was inside, rather than on the surface of, the cells at that timepoint. A typical result is shown in **panel B**; the cell on the left was not transfected, whereas the cell on the right demonstrates a diffuse intracellular signal, rather than a surface pattern. We assessed several siRNAs, and focused on two that were effective in experiments with adequate transfection efficiency. Reduction in S14 mRNA by two siRNAs, as assessed by RT-RT-PCR analysis of R5020-treated T47D cells 48 h after transfection is shown in **panel C**. Cyclophilin mRNA was employed as a reference sequence, and did not vary among treatments. Western analysis of cell lysates at the

48 h post-transfection timepoint demonstrated that siRNA (in this instance siRNA #1) effected the desired knockdown of S14 protein, as expected from the mRNA data (**panel D**).

Thus convinced of the feasibility of the siRNA strategy, we used it to address two aspects of S14 action in breast cancer cells. First we assessed the effect of siRNA on T47D cell accumulation. Results of a timecourse experiment are shown in **Fig. 10, panel A**. Cells accumulated in the presence of the control siRNA, whereas significant cell dropout was observed in the presence of the siRNA. A comparable effect was observed with another S14-siRNA. We also examined the prediction that a reduction in S14 expression would abrogate the induction of FAS mRNA by progestin. Real time-RT-PCR analysis of the same RNA represented in Fig. 8, panel C using FAS-specific primers demonstrated a significant reduction in FAS message in response to S14 siRNAs within 48 h post-transfection (**Fig. 10, panel B**).

In view of recent recognition of nonspecific effects of siRNAs [31], we tested the effect of adenovirus harboring S14 cDNA in the antisense orientation to determine if the effect of siRNA on T47D cell growth would be observed when using this alternative technique. Growth of cells exposed to the control virus did not differ from the uninfected group 120 h after infection (**Fig. 11, panel A**). Inspection showed that a major cell dropout began in the Ad-S14-AS group ~96 h after infection, and this was confirmed by the MTS assay (data not shown). An *in situ* TUNEL assay 96 h postinfection showed evidence of apoptosis in the antisense-treated group at that timepoint (**panel B**). Apoptotic effects of Ad-S14-AS were also seen in MCF7 and SKBR3 breast cancer cells, whereas the antisense adenovirus had no effect on the accumulation of

HepG2 cells (data not shown). We assessed the lipid synthetic rate of the cells 48 and 24 h before the onset of apoptosis (48 and 72 h postinfection, respectively) (**panel C**). Incorporation of labeled acetate into lipids was not different among the groups 48 h postinfection, whereas a sharp reduction was seen in antisense-treated wells 24 h later.

We performed analogous studies using siRNA transfection in MCF10a cells, a nontumorigenic human mammary epithelial line that expresses low levels of lipogenic enzymes and is not susceptible to killing by FAS enzyme inhibition as are transformed MCF10a or breast cancer cell lines [32]. FACS analysis 4 h after transfection using fluorescent siRNA showed that MCF10a cells were transfectable (**Fig. 12, panel A**). We compared T47D and MCF10a cell content of S14 and FAS mRNAs (**panels B, C**). Levels of both messages were so low that some wells yielded no signal. In contrast to T47D cells, MCF10a cell growth was not affected by S14 siRNA (**panel D**). In order to further compare the phenotypes of the T47D and MCF10a cells, we exposed both cell lines to the fatty acid synthase inhibitor cerulinen (10 μg/ml x 48 h; **panel E**). This confirmed previous reports of the differential sensitivity of the lines to inhibition of lipogenesis [5, 32].

Discussion

The tumorigenic potential of progestin was highlighted in the Women's Health Initiative, where chronic administration of estrogen plus progestin, but not estrogen alone, was associated with a significant increase in breast cancer risk [33]. In progesterone receptor-expressing MCF7 and T47D breast cancer cells, progestin induces lipogenesis-related mRNAs, including FAS and S14

[34] [15]. In the current study we directly assessed the role of SREBP-1 in the regulation of S14 mRNA and protein, determined consequences of raising or lowering S14 expression in T47D breast cancer cells, and compared nontumotigenic MCF10a mammary epithelial cells to the mammary cancer cells with respect to S14 expression.

We analyzed S14 gene expression because of its role in lipogenesis in normal and malignant mammary cells ([2]; reviewed in [1]). S14 is highly expressed in lactating human mammary epithelium [2], and lactating mice with a partial S14 gene knockout exhibit reduced milk fat production [35]. S14 is overexpressed in most breast cancers, to a level approximating that found in lactating mammary epithelium. In some cases this is attributable to gene amplification. The S14 gene lies at the telomeric extremity of the 11q13 cancer amplicon [2], while the centromeric end harbors the cyclin D1 locus. Cyclin D1 is a well-characterized, but long-latency mammary oncogene in mice [36] that is overexpressed in up to half of human breast cancers [37].

These studies confirm previous reports of FAS and S14 gene induction by progestin in breast cancer cells [34] [15]. We found that SREBP-1c mRNA was increased by the steroid as well. SREBP-1c gene expression has been shown to be inducible in other circumstances, including stimulation by insulin and high glucose in rat hepatocytes [16], by refeeding in mouse liver and adipocytes [38], and by androgen in prostate cancer cells [14]. States of increased SREBP-1c action result in enhanced turnover of the extranuclear precursor [39], and it appears logical that augmented production is required to maintain an activated steady state.

A major finding in the current study was that inhibition of SREBP-1c reduced the capacity of progestin to enhance S14 and FAS mRNA expression, thus providing direct evidence for its requirement in the action of the hormone in breast cancer cells. Abrogation of progestin-induced FAS reporter gene activity in the construct lacking the sterol response element was consistent with this conclusion. Conversely, a constitutively active SREBP-1c mutant increased expression of the endogenous S14 and FAS genes in T47D breast cancer cells in the absence or presence of progestin. In the presence of hormone, striking superinduction of both mRNAs was observed with concurrent SREBP-1c stimulation.

The superinduction of S14 cannot be ascribed to enhancement of any component of the SREBP-1c activation apparatus, such as SREBP cleavage activating protein (SCAP), as was demonstrated for FAS gene expression in androgen-stimulated prostate cancer cells [14]. The adenoviral construct we used codes for the mature form of SREBP-1c, and thus does not require proteolytic processing. We therefore surmise that, while SREBP-1c is required for full induction of S14 mRNA by progestin, the hormone does not signal through that transcription factor directly. Rather, we propose that SREBP-1c acts in tandem with another factor that directly transduces progestin-mediated amplification of the SREBP-1c signal.

We examined T47D cells for the presence of two potential mediators of the observed superinduction. The amplified signal could not be attributed to progestin induction of PPAR Gamma Coactivator-1ß (PGC-1ß), an inducible protein that can directly coactivate nuclear SREBP-1c in hepatocytes [40], because we did not find expression of PGC-1ß mRNA in T47D cells.

In hepatocytes, induction of lipogenic gene expression requires the presence of two distinct signals, one triggered by insulin, and the other by glucose metabolism [8]. Insulin signals through SREBP-1c, and glucose metabolism is sensed by a liver-specific carbohydrate-responsive factor termed carbohydrate response element-binding protein (CHREBP) [41]. Enhanced glucose uptake and glycolysis are hallmarks of cancer (reviewed in [42]), but little is known about glucose signaling to the genome in cancer cells. We found CHREBP mRNA to be readily detectable in a variety of tumor-derived cells, but not in nonlipogenic HeLa and MCF10a cells. Infection of breast cancer cells with a dominant negative Mlx mutant known to disrupt CHREBP signaling in hepatocyes ([30], kindly supplied by H. Towle, U. MN) caused dramatic disruption of cell architecture and cell dropout, consistennt with the hypothesis that CHREBP signaling is an important mediator of lipogenic breast cancer cell survival. As Mlx may interact with factors other than CHREBP [43], we conservatively interpret this experiment as one that failed to establish the null hypothesis that disruption of CHREBP action would *not affect* T47D cell survival. Of note, the Mlx dominant negative mutant does not affect the survival of rat hepatocytes (H. Towle, personal communication). Further work will determine the significance of glucose signaling through CHREBP in breast cancer cells.

Our data provide two independent lines of evidence indicating that effects of progestin on the S14 and FAS genes are indirect. First is the lag-time in accumulation of the mRNAs. This could reflect the time required to induce and activate SREBP-1c and/or other mediators such as CHREBP. Heemers and coworkers observed a lag time for S14 mRNA accumulation in R1881-treated T47D cells comparable to our result [14]. Using a nuclear run-on assay, Joyeux and

coworkers showed that progestin activates FAS gene transcription in T47D cells without detectable lag time [34]. We cannot explain this discrepancy. Second, our transfection experiments demonstrated that progestin-induced S14 and FAS mRNA accumulation is attributable to increased gene transcription, although the promoter fragments in the reporter constructs do not contain recognized progesterone response elements [24].

Our data are the first to examine S14-RP gene expression in cancer cells. S14-RP was not induced by progestin, and did not form multimers with S14. Thus, the peptides appear to be distinct from standpoints of regulation and physical interaction. Importantly, S14-RP did not protect T47D cells from S14 siRNA- or S14 antisense-mediated demise.

We used adenoviral gene delivery to enhance, and siRNA transfection and RNA antisense to reduce, S14 expression in T47D cells. One must interpret siRNA experiments with caution in view of recent evidence of nonspecific effects on bystander genes (reviewed in [31]). We performed control experiments, including quantitation of siRNA transfection efficiency, verification of localization of the siRNA to the interior of the cells, using more than one siRNA, and the customary use of an irrelevant siRNA. We also exposed non-lipogenic cell types to the siRNAs and antisense. With these multiple controls and the potential caveats in mind, the fluctuations of S14 expression were always accompanied by concordant changes in the accumulation of T47D cells, supporting the hypothesis that S14 facilitates breast cancer cell growth and/or survival. Moreover, expression of FAS mRNA was reduced in cells treated with S14-siRNA, as we previously observed in rat hepatocytes treated with S14 antisense oligonucleotides [44, 45].

Taken together, these observations are consistent with amplification of the S14 gene observed in some breast cancers and S14 protein overexpression seen in the majority of cases [2]. Moreover, our recent immunohistochemical analysis of S14 expression in 131 breast cancer cases demonstrated striking relationships between the intensity of S14 staining and tumor grade and size, as well as disease-free survival that were not seen with other markers [3]. The results of the current tissue culture studies are therefore in harmony with data derived from actual tumors.

This contrasts starkly with a recent report describing S14 action in MCF7 and T47D breast cancer cells [46]. Based on studies of cells overexpressing S14 from stably transfected constructs, the authors concluded that S14 was, in essence, a tumor suppressor that antagonized cell growth, promoted cell death, and enhanced cellular differentiation. We were perplexed by the dissonance between that model and the results of the current studies. Furthermore, the variance between those conclusions and the pathobiology of more than 150 cases of actual human breast cancer that we have assessed for S14 expression to date [2][Wells, 2005 #650] provokes questions about the fidelity of that model.

In summary, we have confirmed that S14 is a progestin-responsive gene in breast cancer cells, and shown that the S14-related peptide gene is not. A new antibody allowed demonstration that changes in S14 mRNA are reflected in levels of the protein. For the first time, we directly demonstrated in mechanistic experiments that full induction of the S14 gene by progestin requires SREBP-1c. Importantly, the hormone appears to amplify the signaling of mature SREBP-1c through an indirect mechanism that does not involve induction of PGC-1ß, but may

require CHREBP. Increased and reduced S14 protein expression effected concordant changes in the growth of breast cancer cells, as predicted from an accumulating mass of data derived from the study of S14 expression in clinical tumors. We propose that S14 and associated components of the lipid synthetic pathway in breast tumors may present attractive therapeutic targets.

Acknowledgements- This work was supported by N.I.H. grant DK58961 and Department of Defense Grant DAMD17-03-1-0544 (to W. B. K.). The opinion or assertions contained herein are the private views of the authors and are not to be construed as official or as reflecting the views of the Department of the Army or the Department of Defense.

References

1. Cunningham, B., et al., *"Spot 14" protein: a metabolic integrator in normal and neoplastic cells.* Thyroid, 1998. 8: p. 815-825.
2. Moncur, J., et al., *The "spot 14" gene resides on the telomeric end of the 11q13 amplicon and is expressed in lipogenic breast cancers.* PNAS, 1998. 95: p. 6989-6994.
3. Wells, W., et al., *Expression of "Spot 14" (THRSP) predicts disease free survival in invasive breast cancer: immunohistochemical analysis of a new molecular marker.* SUBMITTED, 2005.
4. Kuhajda, F., *Fatty-acid synthase and human cancer: New perspectives on its role in tumor biology.* Nutrition, 2000. 16: p. 202-208.
5. Pizer, E., et al., *Inhibition of fatty acid synthesis induces programmed cell death in human breast cancer cells.* Cancer Res., 1996. 56: p. 2745-2747.
6. Pizer, E., et al., *Inhibition of fatty acid synthesis delays disease progression in a xenograft model of ovarian cancer.* Cancer Res., 1996. 56: p. 1189-1193.
7. Kridel, S., et al., *Orlistat is a novel inhibitor of fatty acid synthase with antitumor activity.* Cancer Res., 2004. 64: p. 2070-2075.
8. Foretz, M., et al., *Sterol regulatory binding protein-1c is a major mediator of insulin action on hepatic expression of glucokinase and lipogenesis-related genes.* PNAS, 1999. 96: p. 12737-12742.
9. Rawson, R., *The SREBP pathway- insights from insigs to insects.* Nature Reviews Molecular Cell Biology, 2003. 4: p. 631-640.
10. Yang, Y., et al., *Regulation of fatty acid synthase expression in breast cancer by sterol regulatory element binding protein-1c.* Exp. Cell Res., 2003. 282: p. 132-137.
11. Li, J., et al., *Sterol regulatory element-binding protein-1 participates in the regulation of fatty acid synthase expression in colorectal neoplasia.* Exp. Cell. Res., 2000. 261: p. 159-165.
12. Swinnen, J., et al., *Coordinate regulation of lipogenic gene expression by androgens: evidence for a cascade mechanism involving sterol regulatory element binding proteins.* PNAS, 1997. 94(11/97): p. 12975-12980.
13. Swinnen, J., et al., *Stimulation of tumor-associated fatty acid synthase expression by growth factor activation of the sterol regulatory element-binding protein pathway.* Oncogene, 2000. 19: p. 5173-5181.
14. Heemers, H., et al., *Androgens stimulate lipogenic gene expression by activation of sterol regulatory element-binding protein cleavage activating protein/sterol regulatory element-binding pathway.* Mol. Endocrinol., 2001. 15: p. 1817-1828.
15. Heemers, H., et al., *Progestins and androgens increase expression of spot 14 in T47-D breast tumor cells.* BBRC, 2000. 269: p. 209-212.
16. Foretz, M., et al., *Add1/SREBP-1c is required in the activation of hepatic lipogenic gene expression by glucose.* Mol. Cell. Biol., 1999. 19: p. 3760-3768.
17. Kinlaw, W.B., P. Tron, and A.S. Friedmann, *Nuclear localization and hepatic zonation of rat "spot 14" protein: immunohistochemical investigation employing anti-fusion protein antibodies.* Endocrinol., 1992. 131: p. 3120-3122.
18. Mizuguchi, H. and M. Kay, *Efficient construction of a recombinant adenovirus vector by an improved in vitro ligation method.* Human Gene Therapy, 1998. 9: p. 2577-2583.
19. Shimomura, I., et al., *Differential expression of Exons 1a and 1c in mRNAs for sterol regulatory element binding protein-1 in human and mouse organs and cultured cells.* J. Clin. Invest., 1997. 99: p. 838-845.

20. Field, F., et al., *Regulation of sterol regulatory element-binding proteins by cholesterol flux in CaCo-2 cells.* J. Lipid Res., 2001. 42: p. 1687-1698.
21. Chalbos, D., et al., *Fatty acid synthase and its mRNA are induced by progestins in breast cancer cells.* J. Biol. Chem., 1987. 262: p. 9923-9926.
22. Oskouian, B., *Overexpression of fatty acid synthase in SKBR3 breast cancer cell line is mediated via a transcriptional mechanism.* Cncer Letters, 2000. 149: p. 43-51.
23. Campbell, M., G. Anderson, and C. Mariash, *Human spot 14 glucose and thyroid hormone response: characterization and thyroid hormone response element identification.* Endocrinol., 2003. 144: p. 5242-5248.
24. Lieberman, B., et al., *The constitution of a progesterone response element.* Mol. Endocrinol., 1993. 7: p. 515-527.
25. Wang, X., et al., *Duplicated spot 14 genes in the chicken: characterization and identification of polymorphisms associated with abdominal fat traits.* Gene, 2004. 332: p. 79-88.
26. Anderson, G., et al., *The spot-14 related proteins regulate de novo lipogenesis and resitance to diet-induced obesity.* Endocrine Society annual meeting, New Orleans LA, June 19, 2004, 2005. Abstract 34-2.
27. Cunningham, B., et al., *"Spot 14" Protein-Protein Interactions: Evidence for both Homo- and Heterodimer Formation in vivo.* Endocrinol., 1997. 138.
28. Dentin, R., et al., *Hepatic glucokinase is required for the synergistic action of CHREBP and SREBP-1c on glycolytic and lipogenic gene expression.* J. Biol. Chem., 2004. 279: p. 20314-20326.
29. Stoeckman, A., L. Ma, and H. Towle, *Mlx is the functional heteromeric partner of the carbohydrate response element-binding protein in glucose regulation of lipogenic enzyme genes.* J. Biol. Chem., 2004. 279: p. 15662-15669.
30. Ma, L., N. Tsatsos, and H. Towle, *Direct role of CHREBP-Mlx in regulating hepatic glucose-responsive genes.* J. Biol. Chem., 2005. 280: p. 12019-12027.
31. Jackson, A. and P. Linsley, *Noise amidst the silence: off-target effects of siRNAs?* Trends in Genetics, 2004. 20: p. 521-524.
32. Yang, Y., et al., *Activation of fatty acid synthase during neoplastic transformation: role of mitogen-activated protein kinase and phophatidylinositol 3-kinase.* Exp. Cell Res., 2002. 279: p. 80-90.
33. Roussouw, J., G. Anderson, and R. Prentice, *Risks and benefits of estrogen plus progestin in healthy postmenopausal women: principal results from the Women's Health Initiative randomized controlled trial.* JAMA, 2002. 288: p. 321-333.
34. Joyeux, C., H. Rochefort, and D. Chalbos, *Progestin increases gene transcription and messenger ribonucleic acid stability of fatty acid synthetase in breast cancer cells.* Mol. Endocrinol., 1989. 4: p. 681-686.
35. Zhu, Q., et al., *The spot 14 null mutant mouse exhibits defective mammary gland development in the adult and impaired lipogenesis in the neonate.* Endocrine Society 82nd Annual Meeting, 2000: p. Abstract 1562.
36. Wang, T., et al., *Mammary hyperplasia and carcinoma in MMTV-cyclin D1 transgenic mice.* Nature, 1994. 369(6/23): p. 669-671.
37. Bartkova, M., et al., *Cyclin D1 protein expression and function in human breast cancer.* Int. J. Cancer, 1994. 57: p. 353-361.

38. Kim, J., et al., *Nutritional and insulin regulation of fatty acid synthase and leptin gene expression through ADD1/SREBP1.* J. Clin. Invest., 1998. 101: p. 1-9.
39. Yabe, D., et al., *Liver-specific mRNA for Insig-2 down-regulated by insulin: implications for fatty acid synthesis.* PNAS, 2003. 100: p. 3155-3160.
40. Lin, J., et al., *Hyperlipidemic effects of dietray saturated fats mediated through PGC-1ß coactivation of SREBP.* Cell, 2005. 120: p. 261-273.
41. Yamashita, H., et al., *A glucose-responsive transcription factor that regulates carbohydrate metabolism in the liver.* PNAS, 2001. 98: p. 9116-9121.
42. Dang, C. and S. G., *Oncogenic alterations of metabolism.* TIBS, 1999. 24: p. 68-72.
43. Billin, A., et al., *Mlx, a novel max-like BHLHZip protein that interacts with the Max network of transcriprion factors.* J. Biol. Chem., 1999. 274: p. 36344-36350.
44. Kinlaw, W., et al., *Direct evidence for a role of the "spot 14" protein in the regulation of lipid synthesis.* J. Biol. Chem., 1995. 270: p. 16615-16618.
45. Brown, S.B., M. Maloney, and W.B. Kinlaw, *"Spot 14" protein functions at the pretranslational level in the regulation of hepatic metabolism by thyroid hormone and glucose.* J. Biol. Chem., 1997. 272: p. 2163-2166.
46. Sanchez-Rodriguez, J., et al., *The spot 14 protein inhibits growth and induces differentiation and cell death of human MCF-7 breat cancer cells.* Biochem. J., 2005.

Figure Legends

Fig. 1: Expression of SREBP-1 isoforms in human cancer cells. An ethidium bromide-stained agarose gel is shown. Total RNA was analyzed by RT-PCR. Templates (500 ng) were from HepG2 hepatocarcinoma, T47D lipogenic breast cancer, and HeLa non-lipogenic cervical cancer cells.

Fig. 2: Progestin induces lipogenesis-related mRNAs in T47D cells. Panel A: Data are real time reverse transcriptase PCR analysis of S14, fatty acid synthase, and SREBP-1c mRNA expression, using cyclophilin mRNA as an internal control (data are mean +/- SEM, 6 wells/treatment). Cells were grown in media containing charcoal-stripped fetal calf serum for 48 h, and then exposed to 10 nM R1881 or vehicle for 48 h. Data are arbitrary units, normalized to the cyclophilin signal from each sample. *$p < 0.05$. **Panel B**: Timecourse of S14 and FAS mRNA induction by R5020. Cells were treated as described above and harvested at intervals (4 wells/timepoint). Data (mean +/- SEM, 6 wells/group) for each mRNA are normalized to the initial timepoint.

Fig. 3: Progestin induces S14 and FAS gene transcription. T47D cells were grown in 100 mm plates in stripped fetal calf serum x 48 h, transfected with $S14_{4003}$-LUC (**panel A**) or FAS_{157}-LUC with intact (left) or deleted sterol response element (right) (**panel B**), redistributed into 6 well plates 12 h later, and exposed to 10 nM R1881 or vehicle for 48 h. Equal amounts of cellular protein were analyzed for luciferase activity. Data are mean +/- SEM (6 wells/treatment). *$p<0.05$.

Fig. 4: Effects of SREBP-1c and progestin on S14 mRNA and protein expression. Panel A: S14 mRNA- T47D cells were grown in stripped serum x 48 h and then exposed to adenoviruses (MOI 50) for 1 h. Viruses were 1) ß-galactosidase control (Ad-ß-gal), 2) dominant-negative SREBP-1c (SREBP-1c-DN), and 3) constitutively active SREBP-1c (SREBP-1c). R1881 or vehicle were added to culture media 8 h postinfection, and RNA was harvested 40 h later. Data are real time RT-PCR signals (6/group, mean +/- SEM) corrected for cyclophilin mRNA. * indicates difference between hormone (-) and (+) treatments ($p < 0.05$). **Panel B: S14 protein-** Western analysis of T47D cells treated with R1881, adenovirus harboring a constitutively active SREBP-1c gene mutant, or both. Cells were grown in stripped serum x 48 h, infected with Ad-SREBP-1c or not, and exposed to 10 nM R881 or vehicle for 40 h starting 8 h postinfection. Lysates (50 µg/lane) were analyzed by western blot. The protein migrated at ~ 16 kD.

Fig. 5: S14-RP gene expression in breast cancer cells. Panel A: An ethidium bromide-stained gel of RT-PCR products is shown. Template was total RNA harvested from T47D cells grown in stripped fetal calf serum, and then treated with 10 nM R5020 or vehicle for 48 h. Leftmost lanes show the 132 bp product generated from S14-RP with a primer pair within the coding sequence; the rightmost two lanes show the expected 734 bp product generated with a primer set spanning the entire S14-RP coding region. Negative control was without template. **Panel B:** Real time RT-PCR analysis of the effect of progestin on S14-RP mRNA expression. The same RNA analyzed in panel A was assessed quantitatively, using cyclophilin as control. The difference between treatments is not statistically significant. **Panel C:** Anti-human S14 monoclonal antibody does not recognize S14-RP. Western blots are shown. Extracts (50 µg

protein/lane) of HEK293 cells transfected with a plasmid harboring a HA-tagged full length S14-RP cDNA were analyzed with anti-HA- (left blot) or anti-hS14 monoclonal antibody. HA-tagged S14-RP was detected by the anti-HA, but not the anti-hS14, antibody. Y and N denote yes and no.

Fig. 6: Effects of SREBP-1c and progestin on FAS mRNA. T47D cells were treated as described in the legend to figure 4. Data are real time RT-PCR signals (6/group, mean +/- SEM) corrected for cyclophilin mRNA. * indicates difference between hormone (-) and (+) treatments ($p < 0.05$).

Fig. 7: Interrogation of T47D cells for expression of two candidate mediators of the superinduction of S14 by combined SREBP-1c and progestin stimulation. Ethidium bromide-stained agarose gels of RT-PCR products are shown. **Panel A:** RT-PCR using primers specific for PGC-1ß and templates indicated at the top of the image. A band of the expected size (99 bp) is seen using a plasmid containing the entire PGC-1ß coding sequence as template, but no band was generated from T47D cell RNA. **Panel B:** RT-PCR using primers specific for CHREBP and total RNA from indicated cell lines as template. The panel includes lipogenic mammary cancer (MCF7, SKBR3, ZR75.1, T47D), nonlipogenic breast cancer (MDA-MB-435s), nontumorigenic mammary epithelium (MCF10a), embryonic kidney (HEK293), hepatocarcinoma (HepG2), and nonlipogenic cervical adenocarcinoma (HeLa). The positive control was a plasmid containing CHREBP cDNA. T47D cell data was from a separate gel. **Panel C:** Dominant negative Mlx kills T47D cells. Cells were infected with control or dominant

negative mutant Mlx adenoviruses (MOI 50) and visualized by phase-contrast microscopy 120 h later. Antagonism of Mlx caused gross distortion of cellular architecture and cell dropout.

Fig. 8: Overexpression of S14 accelerates the growth of T47D cells. Panel A: Western analysis of rat S14 in cells infected with recombinant adenoviruses. The blot (25 μg protein/lane) was probed with an antibody specific for rat S14. *Lane 1-* hyperthyroid, carbohydrate-fed rat liver (+ control); *lanes 2,3,4-* breast cancer cells infected (3 days) with viruses containing ß-galactosidase, S14 antisense (- controls), and rat S14 sense genes, respectively. **Panel B:** Breast cancer cell accumulation after adenovirus-mediated S14 gene delivery. Cells (6 wells/timepoint) were infected with Ad-ß-gal, or Ad-S14-sense (MOI 50). Growth assays were performed after 5 days, and data were normalized to the ß-gal-infected control group. * different ($p < 0.05$) from the control.

Fig. 9: Introduction of S14 siRNA into T47D cells. Panel A: FACS analysis of T47D cells 4 h after transfection with fluorescently-tagged siRNA, demonstrating transfection efficiency > 90%. **Panel B:** Localization of siRNA to the cell interior 4 h after transfection by confocal laser fluorescence microscopy. The pattern in the cell at right typifies the cellular distribution of fluorescent siRNA seen at that timepoint (original magnification 40x). An untransfected cell is seen at left. **Panel C:** Knockdown of S14 mRNA by siRNAs. Cells were transfected with the control or two S14-targeted siRNAs, and total RNA was harvested 48 h later. Data are real time RT-PCR signals normalized to cyclophilin mRNA (mean +/- SEM, 6 wells/group; *$p<0.05$). **Panel D:** Knockdown of S14 protein by siRNA #1. Lysates were harvested 2 d post-

transfection, and analyzed by western blot using anti-hS14 monoclonal antibody. The ~ 16 kD band seen in the control culture is not present in the cells treated with S14 siRNA.

Fig. 10: Effects of S14 siRNA on T47D cell growth and FAS mRNA expression. Panel A: Cells grown in the presence of 10 nM R5020 were transfected with control or S14#1 siRNAs, and viable cell number per well was assessed at 0, 3, and 5 d afterward in the MTS assay (mean +/- SEM, 6 wells/timepoint). Cell number increased in the control group, whereas it diminished in the S14 siRNA-treated wells over the first 3 days ($p<0.05$); differences within treatment groups between the third and fifth days were not statistically significant. **Panel B:** Effect of S14 siRNA on FAS gene expression. Total RNA harvested 48 h after transfection was analyzed by real time RT-PCR. A significant reduction in FAS mRNA content was observed after treatment with either S14 siRNA ($p<0.05$).

Fig. 11: S14 antisense kills T47D cells. Panel A: Cells were infected with the indicated adenoviruses (MOI 50) and assessed for viability at 120 h. Data are mean +/- SEM (6 wells/treatment). *$p<0.05$ compared to Ad-ß-gal-infected cells. **Panel B:** Control- (Ad-ß-gal-) or S14 anstisense- (Ad-S14-AS)-infected cells were DNA end-labeled in the TUNEL assay 96 h after adenoviral infection, and imaged by fluorescence microscopy. **Panel C:** Lipid synthesis 48 and 72 h after infection with adenoviruses. Cells were infected with adenoviral vectors and incubated for 4 h in the presence of 100 μ Ci/ml 14-[C]-acetate for 4 h, starting at the 48^{th} or 72^{nd} hours post-infection, at which time total lipids were extracted for determination of radioactive incorporation. Data are mean +/- SEM (4 wells/data point). *$p<0.05$ compared to the Ad-ß-gal infected group.

Fig. 12: Comparison of T47D and MCF10a cell lipogenic gene expression and susceptibility to killing by S14 siRNA and FAS inhibition. Panel A: Introduction of siRNA into MCF10a cells. FACS analysis was performed 4 h after transfection of fluorescent siRNA. Transfection efficiency in this experiment was 86%. **Panel B:** S14 mRNA was quantified by real time RT-PCR in R5020-stimulated T47D cells (48 h) or MCF10a cells treated with control or S14 siRNA for 48 h. MCF10a cells express very low levels of S14 mRNA compared to T47D cells ($p<0.05$) that are not measurably affected by S14 siRNA. **Panel C:** FAS mRNA is likewise low in MCF10a cells ($p<0.05$), and not altered by siRNA treatment. **Panel D:** Timecourse of T47D cell accumulation after transfection of control or S14 siRNA#1. S14 siRNA groups are normalized to the mean values of the control siRNA-transfected group using the MTS assay (data are mean +/- SEM. 6 wells/timepoint). There are no significant differences between groups. **Panel E:** Differential susceptibility of T47D and MCF10a cells to killing by FAS enzyme inhibition. Cells (10,000/6 well plate) were treated with 10 μg/ml cerulinen or vehicle. Media were changed daily, and viable cell number/well was measured in the MTS assay (data are mean +/- SEM, 6 wells/group; * denotes $p<0.05$).

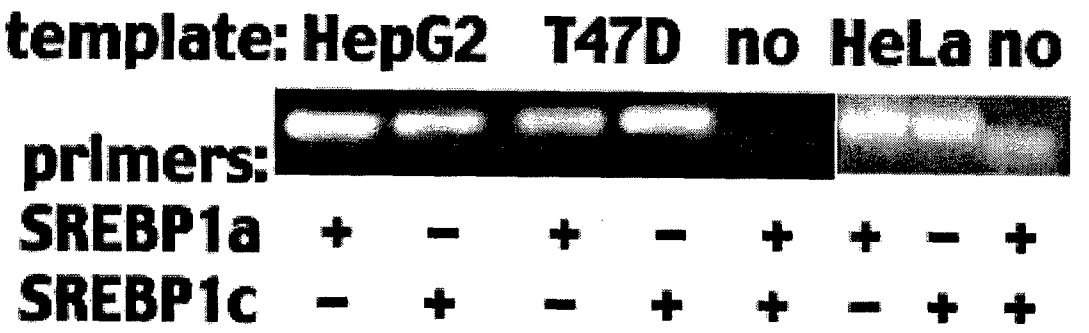

Fig. 1

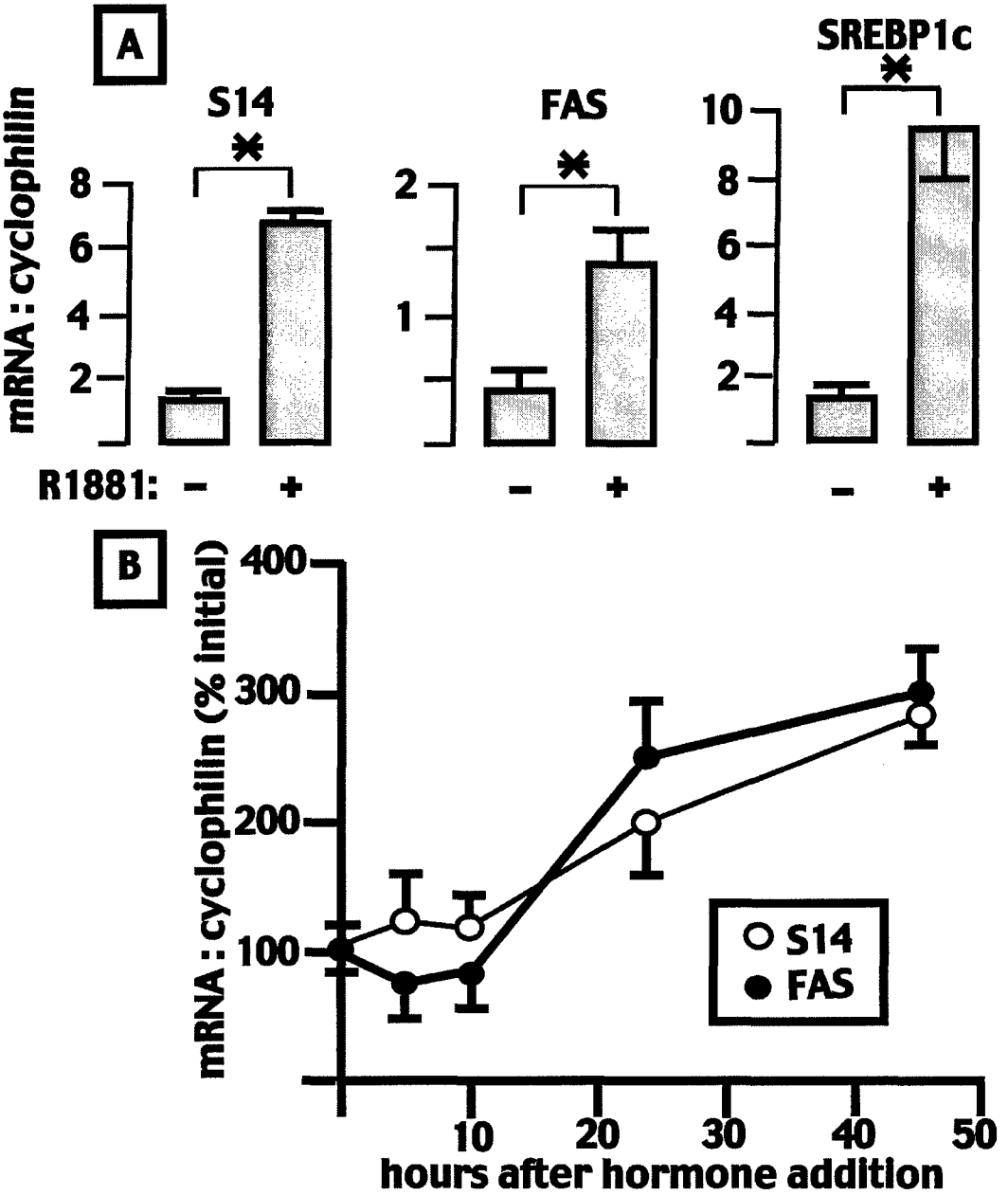
A
S14
FAS
SREBP1c
mRNA : cyclophilin
8
6
4
2
2
1
10
8
6
4
2
R1881: - + - + - +
B
mRNA : cyclophilin (% initial)
400
300
200
100
S14
FAS
10
20
30
40
50
hours after hormone addition

Fig. 2

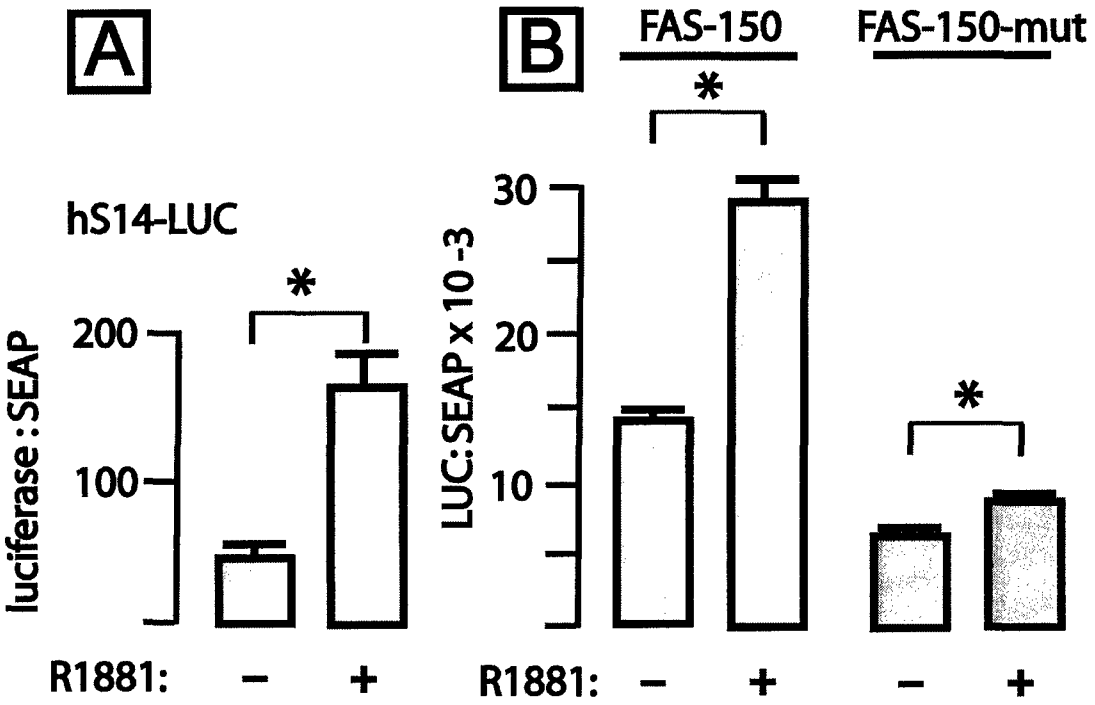
A
hS14-LUC
luciferase : SEAP
200
100
*
R1881:
–
+
B
FAS-150
FAS-150-mut
LUC:SEAP x 10 -3
30
20
10
*
*
R1881:
–
+
–
+

Fig. 3

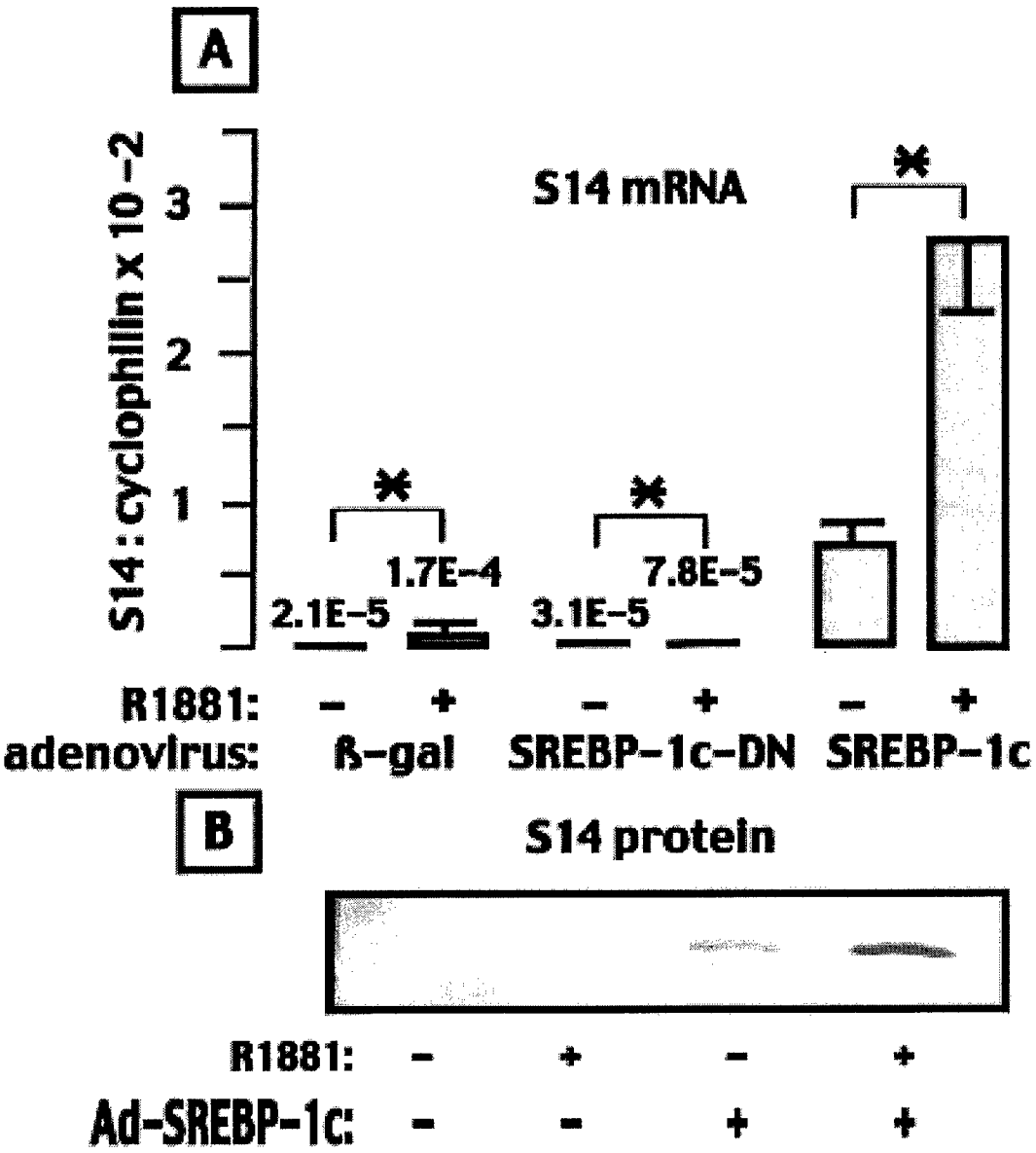
A
S14 mRNA
S14 : cyclophillin x 10 -2
3
2
1
2.1E-5
1.7E-4
3.1E-5
7.8E-5
R1881: - + - + - +
adenovirus: ß-gal SREBP-1c-DN SREBP-1c
B
S14 protein
R1881: - + - +
Ad-SREBP-1c: - - + +

Fig. 4

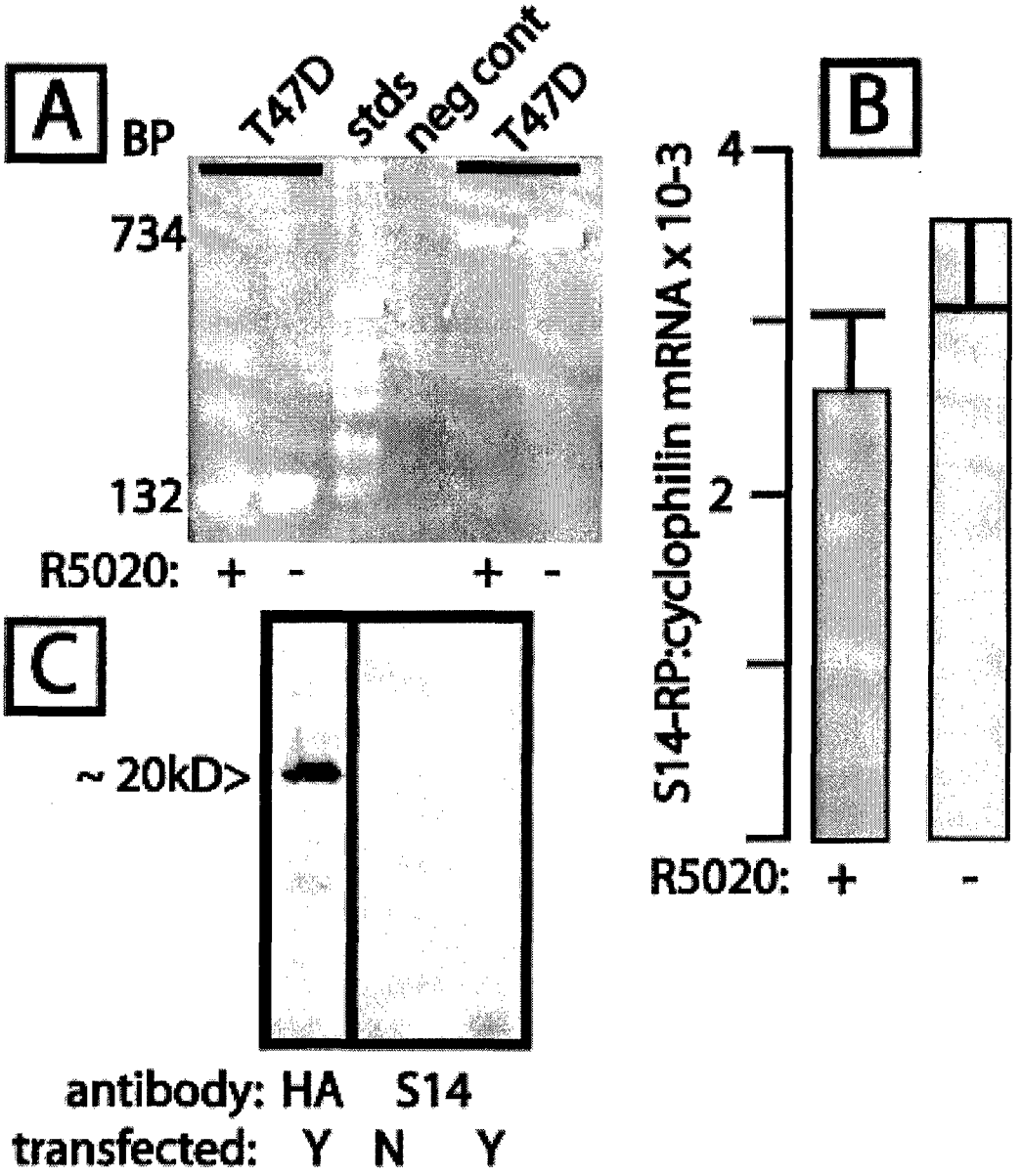
A
BP
T47D
stds
neg cont
T47D
734
132
R5020: + - + -
B
S14-RP:cyclophilin mRNA x 10-3
4
2
R5020: + -
C
~ 20kD>
antibody: HA S14
transfected: Y N Y

Fig. 5

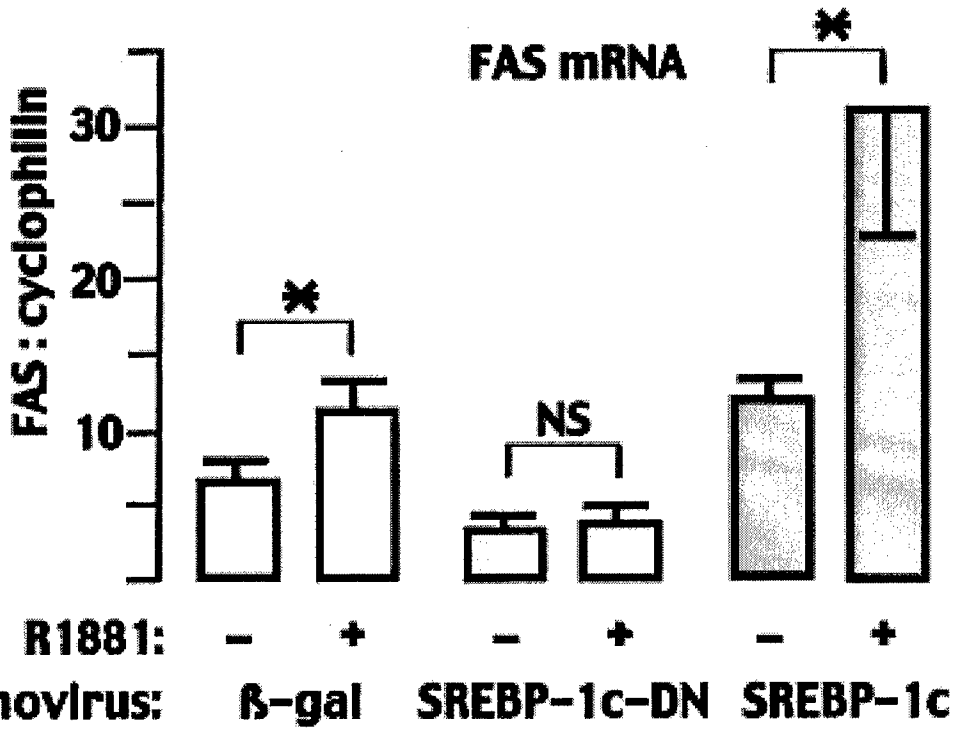
FAS mRNA
FAS : cyclophilin
30
20
10
*
*
NS
R1881: – + – + – +
adenovirus: ß-gal SREBP-1c-DN SREBP-1c

Fig. 6

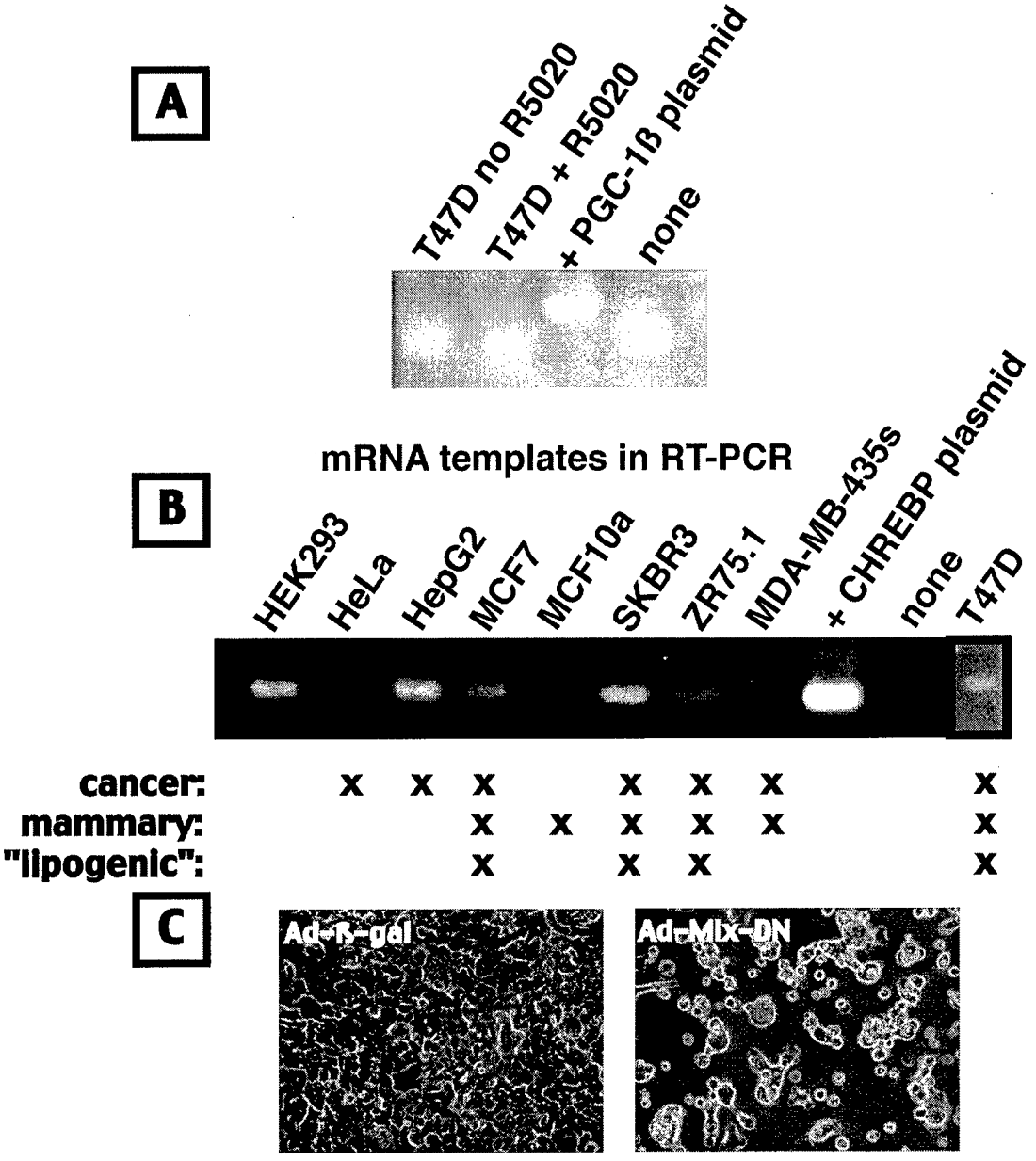
A
T47D no R5020
T47D + R5020
+ PGC-1β plasmid
none
B
mRNA templates in RT-PCR
HEK293
HeLa
HepG2
MCF7
MCF10a
SKBR3
ZR75.1
MDA-MB-435s
+ CHREBP plasmid
none
T47D
cancer:
mammary:
"lipogenic":
C
Ad-β-gal
Ad-Mlx-DN

Fig. 7

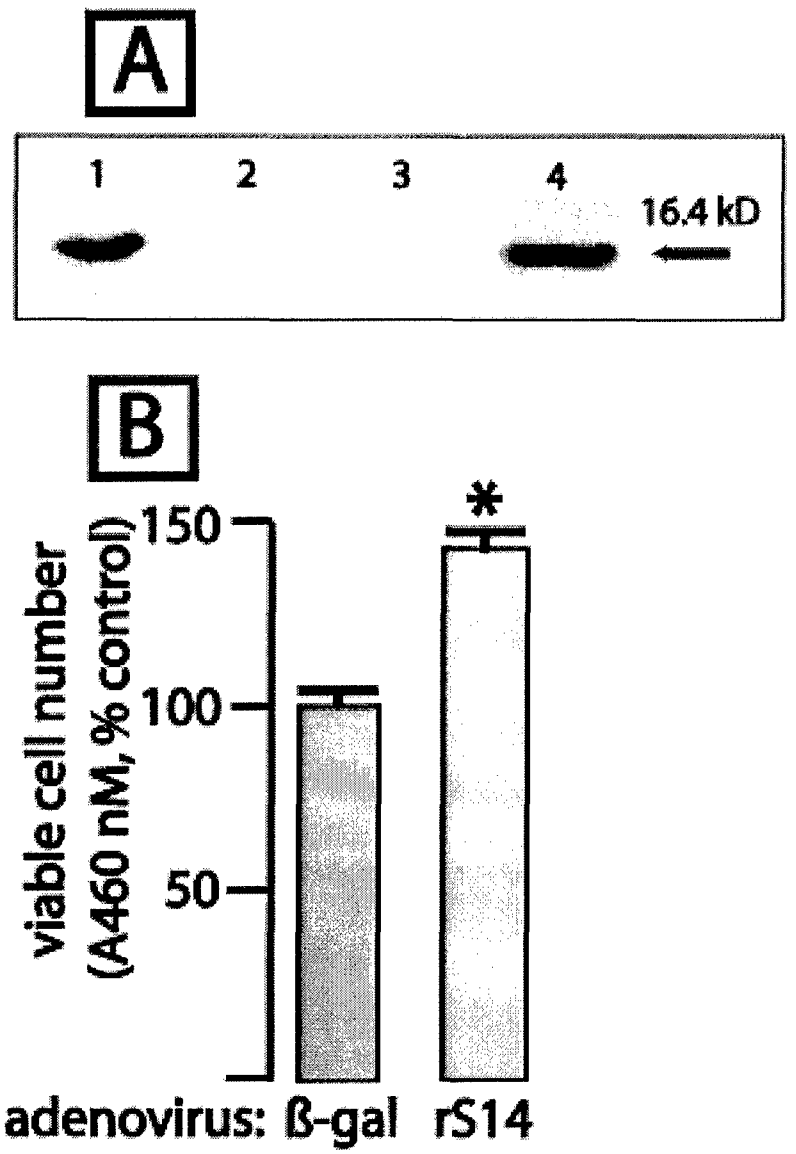
A
1
2
3
4
16.4 kD
B
viable cell number
(A460 nM, % control)
150
100
50
*
adenovirus: ß-gal
rS14

Fig. 8

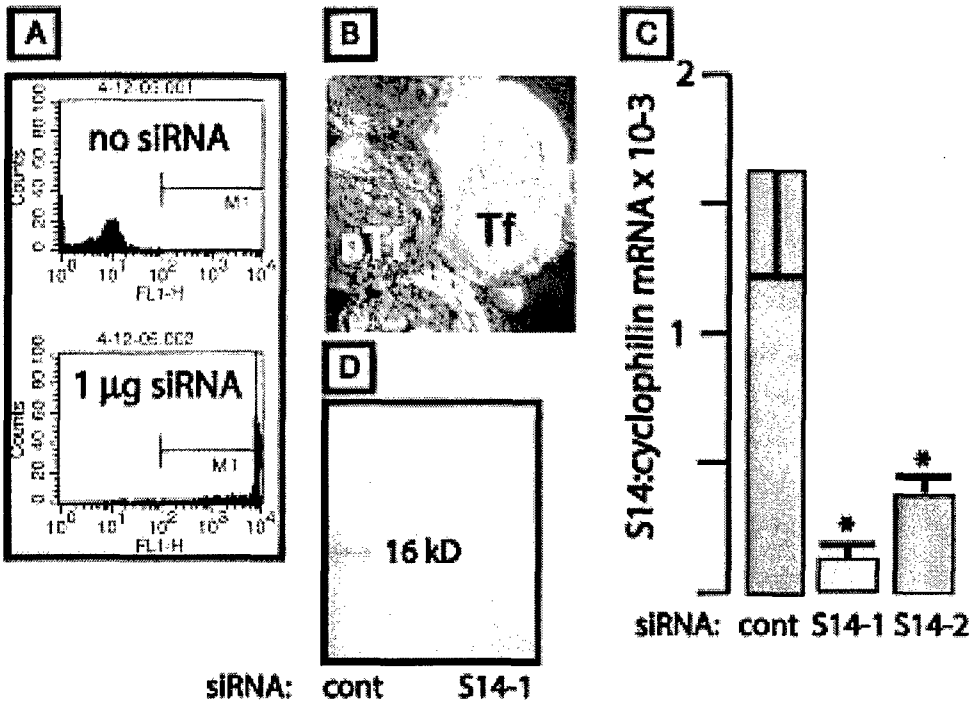
A
no siRNA
1 µg siRNA
Counts
FL1-H
B
Tf
D
16 kD
siRNA: cont S14-1
C
S14:cyclophilin mRNA x 10-3
2
1
*
*
siRNA: cont S14-1 S14-2

Fig. 9

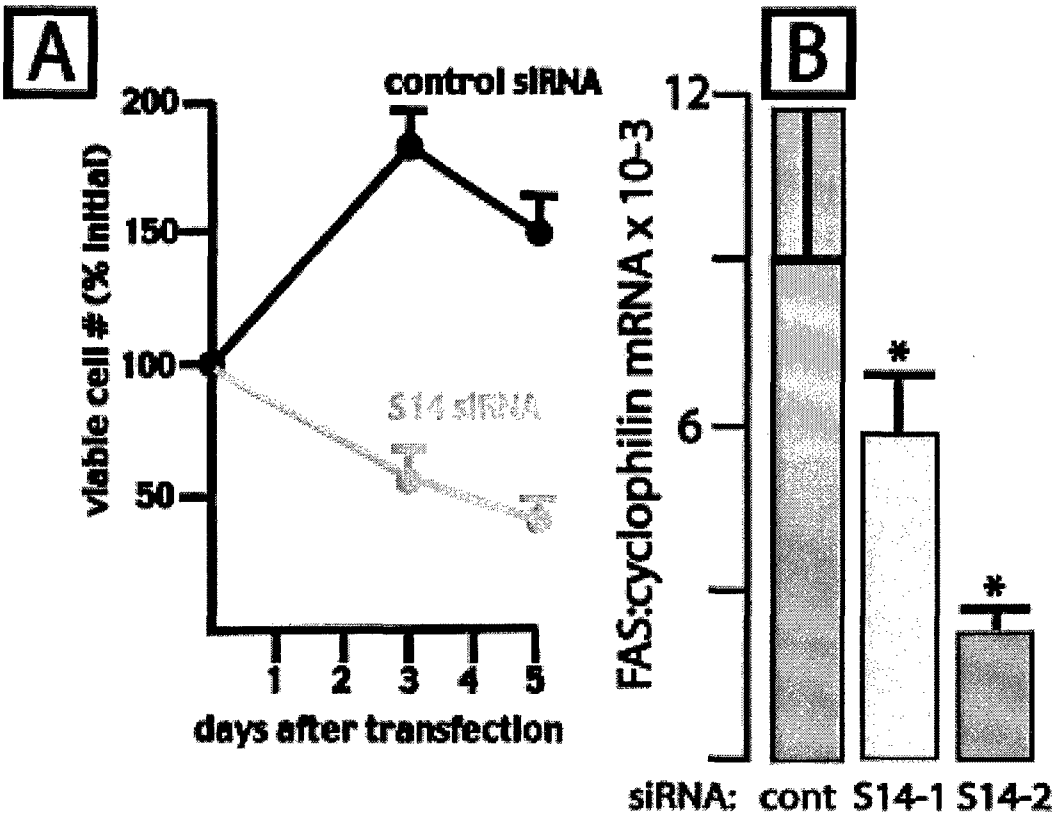
A
control siRNA
S14 siRNA
viable cell # (% initial)
200
150
100
50
1
2
3
4
5
days after transfection
B
FAS:cyclophilin mRNA x 10-3
12
6
*
*
siRNA: cont S14-1 S14-2

Fig. 10

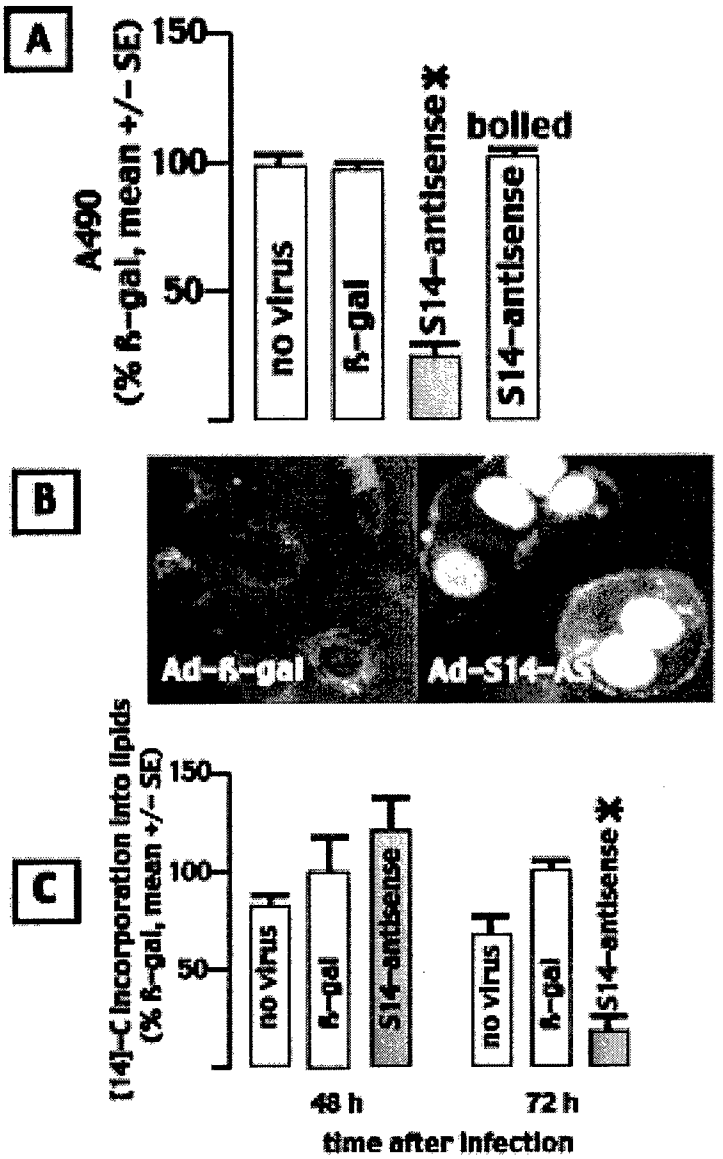
A
A490
(% ß-gal, mean +/- SE)
150
100
50
no virus
ß-gal
S14-antisense *
boiled
S14-antisense
B
Ad-ß-gal
Ad-S14-AS
C
[14]-C incorporation into lipids
(% ß-gal, mean +/- SE)
150
100
50
no virus
ß-gal
S14-antisense
no virus
ß-gal
S14-antisense *
48 h
72 h
time after infection

Fig. 11

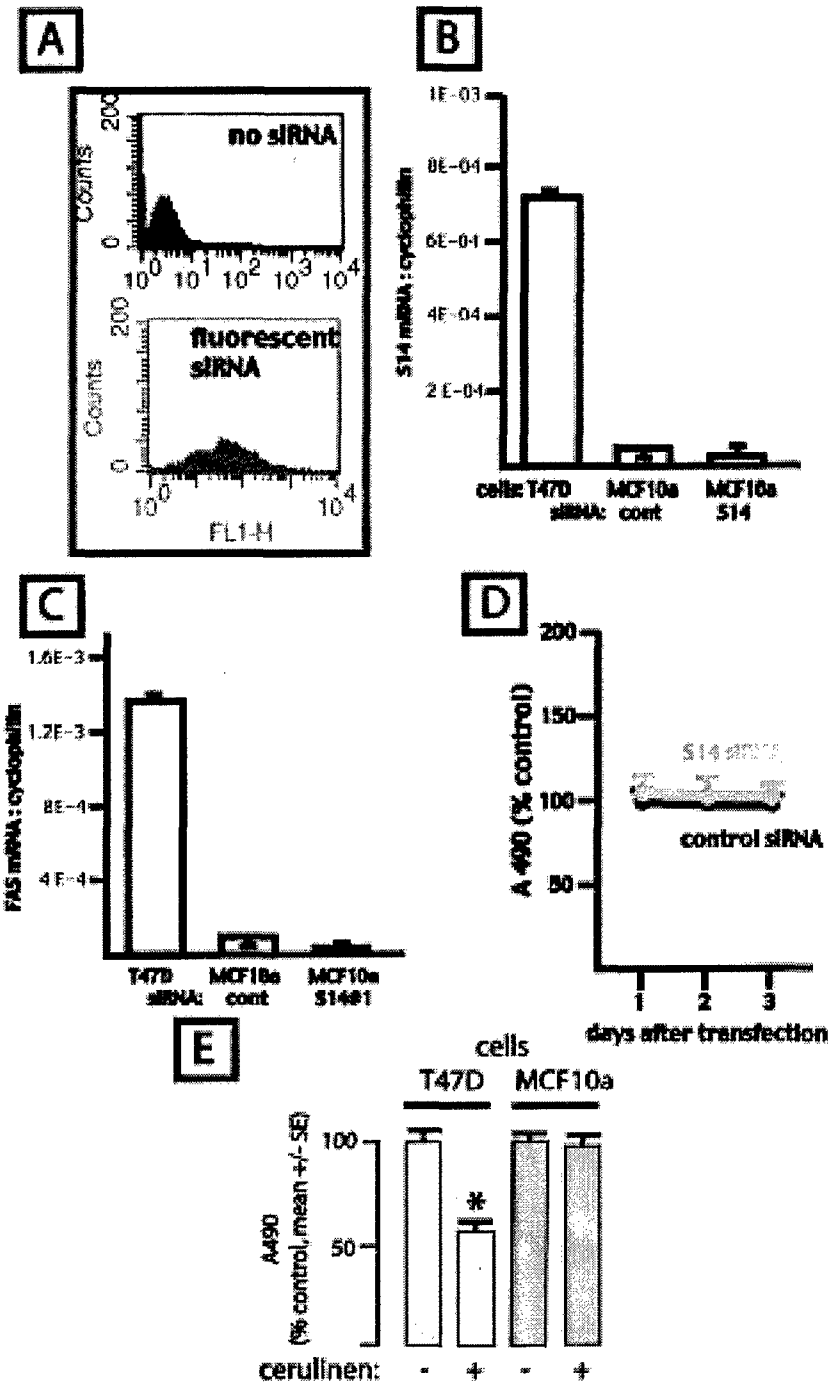
A
no siRNA
fluorescent siRNA
Counts
FL1-H
B
S14 mRNA : cyclophilin
cells: T47D MCF10a MCF10a
siRNA: cont S14
C
FAS mRNA : cyclophilin
T47D MCF10a MCF10a
siRNA: cont S14#1
D
A 490 (% control)
control siRNA
days after transfection
E
cells
T47D MCF10a
A490 (% control, mean +/- SE)
cerulinen: - + - +

Fig. 12

Kinlaw, William B. Appendix item #2

Expression of "Spot 14" (THRSP) predicts disease free survival in invasive breast cancer: immunohistochemical analysis of a new molecular marker

Wendy A. Wells [a,b], Gary N. Schwartz [c,b], Peter M. Morganelli[b,e], Bernard F. Cole, Jennifer G. Chambers [d,b], and William B. Kinlaw [c,b]

Dartmouth Medical School, Departments of Pathology [a], Medicine [c], Community and Family Medicine [d], and the Norris Cotton Cancer Center [b], Lebanon, NH, and US Department of Veterans Affairs, VA Hospital, White River Jct., VT[e]

Address correspondence to:
William B. Kinlaw, MD
606 Rubin Building
1 Medical Center Drive
Lebanon, NH 03756

william.kinlaw@hitchcock.org
Keywords: lipogenesis, gene amplification, chromosome 11q13, tumor markers

Abbreviations used: DCIS, ductal carcinoma in situ; ER, estrogen receptor; FAS, fatty acid synthase; FISH, fluorescent *in situ* hybridization; PCR, polymerase chain reaction; PgR, progesterone receptor; S14, spot 14; THRSP, thyroid hormone-responsive spot 14 protein.

Abstract

Background

Most breast cancers are "lipogenic", defined by high fatty acid synthase (FAS) content and dependence on fatty acid synthesis for growth and survival. S14 (Spot 14; THRSP) is an inducible nuclear protein that activates genes required for fatty acid synthesis. The S14 gene is amplified in ~15% of breast cancers, but clinical correlates of its expression were unknown.

Methods

We analyzed 131 breast cancers diagnosed in 1997-98. Immunhistochemical staining for S14 and FAS was graded 0, 1, or 2+, and the scores were correlated with traditional tumor markers, histological features, and outcome.

Results

S14 and FAS staining were related to tumor size ($p=0.05$ for S14, $p= 0.038$ for FAS), but not to stage. S14 but not FAS scores correlated with tumor grade in both DCIS ($p=0.003$) and invasive cases ($p<0.001$). Invasive cases (pooled node – and +) with weak S14 staining ($n = 21$) showed no recurrence over 3000 d follow-up, including 10 cases with lymph node involvement, whereas 32% of 67 strongly-staining tumors recurred (log rank $p<0.0001$). S14 scores did not cosegregate with other markers, including sex steroid receptors, Her2/neu, and cyclin D1.

Conclusions

Tumor content of S14, a marker of tumor metabolism, increases with histological grade in both DCIS and invasive breast cancer. Low level S14 expression is associated with prolonged disease-free survival in invasive cases, including those with nodal metastasis. High-level expression of S14 identifies a subset of high-risk breast cancers that is not specified by analysis

of sex steroid receptors, Her2/neu, or cyclin D1, and provides a molecular correlate to histologic features that predict recurrence.

Introduction

"Spot 14" (THRSP, S14) is a primarily nuclear protein that is associated with fatty acid synthesis, as indicated by its abundance in lipid-synthesizing tissues and rapid regulation by dietary substrates and fuel-related hormones in rodents (reviewed in [1]). Insight into the metabolic function of S14 came from studies of rat hepatocytes, where inhibition of its expression prevented activation of genes coding the enzymes of fatty acid synthesis, including fatty acid synthase (FAS), acetyl CoA-carboxylase, and ATP citrate-lyase [2, 3]. A partial knockout of the S14 gene in the mouse produced a defect in long chain fatty acid synthesis in the lactating mammary gland [4]. Although its biochemical mechanism of action is not known, it is clear that S14 acts to transduce nutrient-related signals to genes involved in lipid metabolism.

The human S14 gene is located on the 11q13 cancer amplicon, where the cyclin D1 mammary oncogene also resides, prompting the hypothesis that increased S14 expression could confer a growth advantage to tumor cells [5]. In a small series of 21 breast cancers, S14 was abundant in most cases, and was expressed concordantly with that of the rate-determining lipogenic enzyme acetyl CoA-carboxylase in tumors, signifying that S14 is a component of the "lipogenic phenotype" in breast cancer.

Kuhajda and coworkers found that a polypeptide termed "OA519" that was overexpressed in aggressive breast cancers was in fact the long chain fatty acid-synthesizing enzyme FAS [6]. A high level of FAS is the hallmark of the lipogenic tumor phenotype, which is frequent in cancers arising in colon, ovary, and prostate, as well as breast (reviewed in [7]). In addition to its prognostic importance, this metabolic feature may have therapeutic implications. Cerulinen, an

inhibitor of FAS, produced apoptosis of both breast cancer cells and human ovarian tumor xenografts in mice [8, 9], thus linking tumor lipogenesis to cancer cell growth and survival. Orlistat, a drug approved for the treatment of obesity, was recently also found to be a FAS inhibitor with antitumor activity in a mouse model of prostate cancer [10]. The lipid synthetic pathway therefore presents a novel therapeutic target in several common human cancers.

We undertook the current study to examine the hypothesis that S14 expression would identify aggressive breast cancer cases. We determined the frequency and graded the intensity of S14 expression in a breast cancer series, and defined its relationship to histologic features, the expression of conventional tumor markers, and clinical outcome. In view of the established link between S14 and fatty acid synthesis, we stained the tumors for FAS. We also analyzed expression of cyclin D1, a recognized mammary oncogene [11], because of its colocalization with S14 on the 11q13 cancer amplicon [5], which suggested that the two gene products could interact functionally to promote tumor virulence.

We found that that S14 is expressed in the majority of breast cancers, both *in situ* and invasive, and that a high content of S14 in invasive tumors is associated with high grade and bulkier disease. The S14 score did not cosegregate with other tumor markers, including sex steroid receptors, Her2/neu, and cyclin D1. A low S14 score identified a novel subset of patients with invasive tumors that did not recur, irrespective of lymph node involvement, whereas maximal S14 expression was strongly predictive of recurrence.

Methods

Patient population- The Comprehensive Breast Program at the Norris Cotton Cancer Center at Dartmouth Medical School manages a database of 700 patients with tissue blocks and blinded demographic information on tumor characteristics including size, histological grade, lymph node status, and expression of conventional tumor markers (estrogen receptor (ER), progesterone receptor (PgR), and Her2/neu). We selected 131 tumors diagnosed in 1997-98 for this study, including 43 consecutive cases of ductal carcinoma *in situ* (DCIS), 34 consecutive cases of node (-) breast cancer, and 54 consecutive cases of node (+) breast cancer, as well as 20 mammary gland samples from women undergoing reduction mammoplasty who had no history of breast cancer (10 pre- and 10 post-menopausal). Use of patient-derived materials and information was approved by the Institutional Review Board.

Characteristics of the patients are compiled in **Table I**. There were 43 patients with ductal carcinoma *in situ* in the panel. Median age at diagnosis was 56 y, the mean tumor size was 18 mm, the majority of tumors were of intermediate grade, and most patients received breast-conserving therapy. The 34 patients with node negative invasive breast cancer had a median age at diagnosis of 54 y. Mean tumor size was 17 mm and three quarters were 2 cm or less. Less than one quarter of the node negative ductal cancers were high grade, and over 80% were hormone receptor positive. Most of these favorable risk node negative patients were treated with breast conserving- and hormonal therapy. On the other hand, node positive patients were younger, with a median age of 51 y, the primary tumors were larger, with a mean size of 36 mm, there was an equal proportion of intermediate and high grade tumors, most were hormone

receptor positive, and nearly one-third were Her-2/neu positive. Most patients with node positive cancer were treated with chemohormonal therapy following mastectomy.

Determination of conventional tumor markers- Based on correlation with standard biochemical assays for sex steroid receptors, immunostaining of tumor cell nuclei for ER and PgR expression was defined as "negative" (no staining); "equivocal" (1-15% tumor cell nuclei staining); and "positive" (>15% tumor cell nuclei staining). Her2/neu surface protein expression was scored immunohistochemically as 0 through 3+, according to adapted criteria defined in the Herceptest™. Score 0 was defined as absent or faint membranous staining in < 33% of tumor cells. Score 1+ was defined as barely perceptible partial membranous staining in > 33% of cells. Score 2+ was defined as weak to moderate staining of the entire plasma membrane in > 33% of the tumor cells. Score 3+ was defined as strong staining of the entire cell membrane in >90% of the tumor cells. We deemed scores of 0, 1+ and 2+ as negative, and a 3+ score to indicate overexpression. In our laboratory, all Her2/neu slides are read by one experienced pathologist, and only 2.5% of cases immunohistochemically scored as 2+ exhibit a positive signal by fluorescent *in situ* hybridization (FISH). In view of the cost of that test and the excellent reproducibility of immunohistochemical analysis for this antigen at our institution, we did not routinely analyze cases graded as 2+ by FISH.

Anti-human S14 antibody production- We generated a monoclonal antibody in the Norris Cotton Cancer Center Antibody Resource using a protocol approved by the Institutional Animal Care and Use Committee. Hybridomas were prepared from splenocytes of mice immunized with glutathione-S-transferase (GST)-tagged human S14 expressed from vector pGEX-3X

(Amersham) in *E. coli*. Female Balb C mice were immunized intraperitoneally with 50 μg GST-S14 mixed in RIBI adjuvant (Sigma), and boosted with 20 μg antigen in adjuvant 3 and 6 weeks later. Splenocytes were fused with NS1 cells (ATCC) 4 d later. Screening was by enzyme-linked immunosorbant assay in wells coated with His_6-tagged S14 expressed in bacteria from vector pROEx-HT (Life Technologies).

Immunohistochemistry- Tissues were fixed in 10% buffered formalin (Biochemical Science Inc, Swedesboro, NJ), dehydrated through graded alcohols, and paraffin embedded. Tissue sections (4 μm) were coated with adhesive (Sta-onTM, Surgipath Medical Industries, Inc, Richmond IL), mounted on glass slides and stained with hematoxylin for initial review. Estrogen receptor protein (ER) and progesterone receptor protein (PR) expression (antibody at 1:10 and 1:40 respectively, from Biogenix, San Ramon, CA with Citra Plus antigen retrieval) and Her2/neu surface protein expression (antibody at 1:20 from Biogenix, San Ramon, CA) with Citra antigen retrieval) were assessed immunohistochemically in the clinical laboratory at the time of diagnosis. S14 was detected with crude supernatant from a hybridoma designated "KvB4" an IgG type 2a, and Citra antigen retrieval. FAS was detected with an affinity-purified rabbit anti-human FAS IgG preparation, (Immuno-Biological Laboratories Co., Gunma Japan) 1:100 at 3 μg/ml with Citra antigen retrieval. Cyclin D1 was detected with a mouse monoclonal antibody, 1:100, from Biocare, Walnut Creek, CA with Borg antigen retrieval according to published data [12]. Tissue sections were deparaffinized with xylene and hydrated through graded alcohols, and mounted on Biogenix Plus slides (San Ramon, CA). Epitope retrieval was carried out in a steamer under pressure, using buffers described above. Slides were rinsed in water, soaked in PBS and immunostained in a BioGenix I-6000 autostainer (San Ramon, CA) using the Biotin-

Streptavidin Amplified system. Identical timing of incubations and washes was used for all cases. Diaminobenzidine was applied for visualization. Slides were counterstained with hematoxylin, dehydrated through graded alcohols and coverslipped with Richard Allen mounting medium (Richard Allen Medical, Richland, MI).

Determination of S14, FAS and cyclin D1- All slides were scored by one pathologist (W.A.W.). For each antibody, 20 randomly chosen cases were reviewed by a second pathologist to confirm reproducibilitiy. S14 and FAS were scored 0 through 2+ according to the intensity of immunostaining (nuclear for S14, cytoplasmic for FAS). Score 0 was defined as no staining; score 1+ was defined as weak, diffuse staining; score 2+ was defined as strong, diffuse staining. Cyclin D1 was scored 0 through 3+ according to the percentage of tumor nuclei staining (irrespective of the intensity), using published criteria [12], as follows: Score 0 was defined as no immunostaining; Score 1+ was defined as <25% of tumor cell nuclei staining; Score 2+ as 25-75% of tumor cell nuclei staining; Score 3+ as >75% of tumor cell nuclei staining.

Statistical analyses of clinical data- Confidence intervals for rates were calculated using exact binomial methods. Comparisons for S14 and cyclin D1 overexpression between groups were performed using Fisher's exact test. We compared time to disease recurrence between groups using Kaplan-Meier survival estimates and the log-rank test. We also used proportional hazards regression to jointly examine the influence of the stage, prognostic factors, and S14 overexpression on the time to recurrence.

Results

Characterization of the S14 antibody- Western analysis of T47D human breast cancer cells after application of multiple stimuli that enhance or reduce S14 gene expression was performed. In each instance this revealed a single band of appropriate mobility (~16 kD), of intensity concordant with levels of S14 mRNA. We specifically excluded the possibility of cross-recognition of S14-related peptide (S14-RP, STRAIT11499). We transiently transfected a hemagglutinen (HA)-tagged full length S14-RP cDNA (OpenBiosystems) into HEK293 cells, and western analysis with anti-HA antibody revealed robust S14-RP expression, whereas no signal was observed with anti-S14 antibody. These data will be published elsewhere [13].

We compared resting and lactating human mammary gland by immunohistochemistry, because lactation is a major stimulus for S14 expression in epithelium of the lobuloalveolar units [5]. Resting mammary showed primarily white adipocytes of the fat pad with strong nuclear and some cytoplasmic staining, whereas the lactiferous duct epithelium was essentially devoid of S14 (**Fig. 1, panel A**). Lactating mammary gland showed strong staining in nuclei and cytoplasm of epithelial cells (**panel B**). Substitution of an irrelevant IgG2A for the first antibody in immunohistochemistry abrogated the signal (not shown). Staining for FAS showed an intense cytoplasmic signal, with sparing of nuclei (**panel C**).

Immunohistochemistry of breast cancer- Examples of DCIS (left panels) and invasive breast cancer (right panels) stained for S14 and FAS are shown in **Fig. 2**. Tumors of either stage yielded no signal when primary antibodies were omitted (upper panels). S14 staining was primarily nuclear, as seen previously in rat liver [14] and human breast cancer [5] using

polyclonal IgG preparations in immunohistochemistry. FAS immunoreactivity was cytosolic, as expected [15].

Frequency of S14 and FAS expression in normal and malignant mammary tissue- S14 and FAS were detectable in essentially all examples of normal mammary gland, DCIS, and invasive breast cancer (**Table II**). The frequency of maximal expression did not vary between DCIS and invasive cancers, and the scores did not differ between invasive cancers with or without lymph node metastases.

Relationship of S14 expression to histological tumor grade and tumor size- The fraction of cases exhibiting maximal staining for S14 was significantly correlated with tumor grade and size (**Fig. 3**). S14 expression in grade 1 DCIS was as likely to be maximal as it was in normal mammary epithelium (**Panel A**), but the prevalence of strong staining increased with advancing grade, to 97% in grade 3 cases ($p=0.003$). In invasive cancers (**Panel B**) a similar relationship was found, with 100% of grade 3 tumors (pooled lymph node negative and positive) exhibiting a maximal score ($p<0.001$). Invasive cancers also exhibited increased S14 expression as a function of tumor size (**Panel C**). Strong staining was found in 58% of tumors < 1.0 cm in size, and increased to 80 and 83% for lesions 1.0-2.0 and > 2.0 cm in diameter, respectively ($p=0.05$).

FAS and tumor size and grade- In DCIS, the relationship between FAS expression and tumor grade approached significance, with grade 1/2/3 cases exhibiting maximal expression in 86/96/100% of cases, respectively ($p=0.08$), consistent with a previous report [16]. No relationship was seen in invasive cases, because essentially all showed maximal expression of

this antigen. As was the case for S14, FAS content correlated with invasive tumor size. Strong staining was found in 88% of tumors < 1.0 cm in size, and increased to 100% for 1.0-2.0 or > 2.0 cm lesions (p=0.04).

Comparison of the expression of S14, FAS, and conventional tumor markers- There was no significant correlation between the expression of S14 and ER or PgR status in either DCIS or invasive cases (for ER, p=0.21/0.54; for PR p=0.56/0.78, respectively). Likewise, there was no association of a positive score for Her2/neu with the S14 or FAS scores in DCIS or invasive breast cancers (for S14, p=0.10/0.10; for FAS p=0.52/0.51, respectively). As expected (reviewed in [17]), Her2/neu amplification did presage reduced disease-free survival in invasive cases (p=0.046).

Cyclin D1- In both DCIS and invasive breast cancer there was no relationship between the S14 score and the level of cyclin D1 expression (p=1.00 and 0.28, respectively). Cyclin D1 staining intensity did not increase with tumor size at either stage (p=0.42, 0.25, respectively). Likewise, Cyclin D1 staining did not correlate with tumor grade in either DCIS or invasive disease. In DCIS, strong staining for cyclin D1 was associated with ER expression (p=0.028). The association of cyclin D1 expression and that of PgR was also statistically significant (p=0.05). In invasive cases, the association between PgR and strong cyclin D1 expression nearly reached significance (p=0.06). We did not find an association of the cyclin D1 score and disease-free survival (p=0.4).

S14 and clinical outcome- Kaplan-Meier analysis of recurrence after primary treatment of invasive tumors (with or without lymph node involvement) revealed a significant relationship ($p=0.015$) between the level of S14 expression in the primary tumor and disease-free survival over the ensuing 3000 days (**Fig. 4**). Indeed, no cases exhibiting a score of 0 or 1+ ($n=21$) recurred, whereas 32% of the 67 tumors with maximal S14 content did. The number of cases at each S14 score precluded multivariate analysis, but there did appear to be an effect of tumor grade independent of the S14 score. Among strongly staining-cases, none of 11 grade I invasive tumors recurred, 2/19 grade 2 tumors recurred, and 12/26 grade 3 tumors did so.

We observed separable effects of the S14 score and the presence of nodal metastases at initial surgery on disease-free survival in invasive disease (**Fig. 5**). Among 34 node-negative cases, there was one recurrence, and it was among the 23 cases with strong S14 expression. Among 10 node positive cases with weak S14 expression, there was no recurrence. In contrast, of the 44 node positive cases with strong staining, 14 (32%) developed recurrent disease (log rank $p<0.0001$).

Discussion

S14 is a primarily nuclear protein found in lipogenic tissues, where it is rapidly regulated by metabolic fuels and fuel-related hormones, as detailed in the introduction. We previously localized the S14 gene to the cancer amplicon at 11q13 and demonstrated that it was overexpressed in most breast cancers, to a level approximating that seen in lactating mammary gland. This suggested that overexpression of S14 could provide an advantage to tumor cells [5]. The concordance of S14 overexpression with that of the pace-setting enzyme of long chain fatty

acid synthesis further established S14 as a component of the "lipogenic" breast cancer phenotype. In the current study we extended the analysis of the frequency and degree of S14 expression in breast cancer, and examined its clinical correlates. Given the poor prognosis observed in tumors with amplification at 11q13 [18, 19], and in tumors with a lipogenic phenotype [15, 20], our major hypothesis was that overexpression of S14 would be associated with virulent tumors.

We were surprised to find detectable S14 in essentially all mammary samples, malignant and benign. Overexpression, as opposed to detectable expression, was also not restricted to malignant or lactating mammary tissue, but was seen in the majority of normal mammary tissue samples, irrespective of menopausal status, and in the majority of tumors, regardless of stage. In tumors, however, brisk expression was strongly related to morphological indices of tumor aggressiveness. The frequency of maximal S14 expression exhibited a strong positive correlation with tumor grade in both *in situ* and invasive cases, and was also associated with larger invasive tumor size. Although we did not analyze metastases, our data indicate that S14 overexpression is not acquired during tumor progression. S14 is therefore a molecular tumor marker that, as for ER and PgR, is also expressed in normal, nonlactating mammary epithelial cells. When overexpressed in tumors, however, S14 is associated with morphological criteria that predict aggressive tumor biology, and most importantly, with reduced disease-free survival.

Based on these findings in breast tumors, and our own observations in breast cancer cells [13], we were perplexed by a recent report suggesting that S14 acts to promote differentiation and apoptotic death of cultured breast cancer cells harboring a stable S14 expression construct [21].

The discrepancy suggests that the tissue culture model employed in those studies may not faithfully reflect human breast cancer biology.

The association of S14 overexpression with histologically-based indices of tumor aggressiveness prompts the question of whether S14 expression would provide a prediction of disease-free survival independent of tumor grade and size. We were unable to answer this important question by performing a multivariate analysis in this study, because of an insufficient number of cases at each S14 grade. A larger analysis will be required to determine whether the histological grade and S14 score are statistically separable. One might expect, however, a tight relationship between the expression level of a useful molecular marker and the morphological criterion of tumor grade. It did appear that an effect of tumor grade was apparent among cases with the highest S14 expression score, because there was a trend for increasing grade to be associated with progressively higher recurrence rates in the 2+ S14 group. S14 expression did exert a significant effect on disease-free survival independent of lymph node status. Remarkably, when the S14 expression score was low there were no recurrences in cases with lymph node metastasis.

Several predictions based on laboratory work were not fulfilled by this study. We hypothesized that S14 overexpression would be associated with PgR. This was based on data indicating that the S14 gene is activated by progestin in breast cancer cells [22], an observation that we have confirmed [13]. We were surprised not to find an association of S14 overexpression with sex steroid receptor expression. We likewise hypothesized that a lipogenic tumor phenotype would be associated with expression of Her2/neu, based on a report of cDNA microarray analysis of

breast cancer cells demonstrating FAS to be a prominent Her2/neu response gene [23]. We did not find a correlation, however, between Her2/neu expression and that of S14 or FAS in tumors.

We predicted S14 expression to correlate with that of cyclin D1. Although both genes are found on the cancer amplicon at 11q13 [24] [25], we did not expect coamplification to be the mechanism for coexpression, because amplification at 11q13 occurs in 15-20% of invasive breast cancers, a much smaller fraction than that exhibiting overexpression of cyclin D1 ([26], reviewed in [27]) or S14 ([5] and the current work). Coamplification of the marker closest to the S14 locus (GARP) and the cyclin D1 gene in many breast cancer cases suggested the possibility of a functional interaction between S14 and the cyclin [28]. We did not, however, find an association between expression of the two genes. The observed association of cyclin D1 overexpression and the presence of ER was consistent with previous reports ([29], reviewed in [27]). Cyclin D1 is a recognized mammary oncogene [11], but the literature is not unanimous regarding its influence on prognosis in breast cancer [30, 31]. In the current study we did not find such a relationship.

S14 expression therefore did not correlate with the conventional markers or cyclin D1, and thus defined a novel subset of patients among those with invasive tumors. Aggressive tumors may select mechanisms other than those mediated by progestin or Her2/neu signaling to activate the S14 gene. This point was emphasized by inspection of the rare examples in our series that did not express ER, PgR, or Her2/neu. Among these six "triple negative" cases, five were strongly positive for S14 and FAS.

Ingestion of a low fat diet may improve the prognosis in breast cancer patients [32]. How might this observation relate to the unfavorable prognosis associated with lipogenic breast tumors? We assume that most of our subjects were ingesting a relatively high fat, westernized diet, and therefore infer that the tumors do not exhibit the downregulation of fatty acid synthesis expected in normal tissues [33]. We speculate that a combined excess of dietary and newly-synthesized long chain fatty acids provides an advantage to tumor metabolism greater than that produced by endogenous synthesis alone. In view of our observation that inhibition of S14 expression caused reduced long chain fatty acid synthesis in hepatocytes [3], we hypothesize that S14, and perhaps other components of the regulatory apparatus of lipid synthesis could present novel therapeutic targets in lipogenic breast cancers, as is the case for FAS itself.

The expression of thousands of genes in human breast cancers and mouse models of the disease have been screened using cDNA microarray technology to identify markers of tumor behavior [34, 35]. These studies did not provide independent information regarding the association of S14 with aggressive breast cancer biology, however, because the S14 (THRSP) cDNA was not dotted on the arrays employed.

In summary, abundant expression of S14 may occur in breast cancers at early and late stages, and brisk expression of S14 is associated with high grade DCIS and with high grade and larger invasive tumors, but not with the status of regional lymph nodes at initial surgery. The strong association of a low S14 score with prolonged disease-free survival in invasive breast cancer may be related to its association with lower histological tumor grade, but S14 had prognostic value independent of lymph node status. S14 expression did not segregate with traditional tumor

markers, and certainly was not associated with differentiated, tractable tumors as inferred from a recent report based on breast cancer cells [21]. S14 is a marker for aggressive mammary tumors that are likely to recur. It appears possible that the intensity of therapy, and its attendant human and financial costs, could be reduced in cases that have low expression of S14. Further study will be required before S14 is factored into clinical decision making in breast cancer.

Acknowledgements- We thank Dr. Vincent Memoli for consultation regarding immunohistochemistry, Ms. Maudine Waterman for performing the immunostaining, and Drs. Murray Korc and Mark Schneider for critical readings of the manuscript.

Grant support- NIH RO1 DK 058961 (to W.B.K.), and U.S. Department of Defense grant DAMD17-03-1-0544 (to W.B.K.).

Literature cited

1. Cunningham, B., et al., *"Spot 14" protein: a metabolic integrator in normal and neoplastic cells.* Thyroid, 1998. **8**: p. 815-825.
2. Kinlaw, W., et al., *Direct evidence for a role of the "spot 14" protein in the regulation of lipid synthesis.* J. Biol. Chem., 1995. **270**: p. 16615-16618.
3. Brown, S.B., M. Maloney, and W.B. Kinlaw, *"Spot 14" protein functions at the pretranslational level in the regulation of hepatic metabolism by thyroid hormone and glucose.* J. Biol. Chem., 1997. **272**: p. 2163-2166.
4. Anderson, G., et al., *The spot-14 related proteins regulate de novo lipogenesis and resitance to diet-induced obesity.* Endocrine Society annual meeting, New Orleans LA, June 19, 2004, 2005. **Abstract 34-2**.
5. Moncur, J., et al., *The "spot 14" gene resides on the telomeric end of the 11q13 amplicon and is expressed in lipogenic breast cancers.* PNAS, 1998. **95**: p. 6989-6994.
6. Kuhajda, F., S. Piantadosi, and G. Pasternack, *Haptoglobin-related protein (Hpr) epitopes in breast cancer as a predictor of recurrence of the disease.* NEJM, 1989. **321**: p. 636-641.
7. Kuhajda, F., *Fatty-acid synthase and human cancer: New perspectives on its role in tumor biology.* Nutrition, 2000. **16**: p. 202-208.
8. Pizer, E., et al., *Inhibition of fatty acid synthesis delays disease progression in a xenograft model of ovarian cancer.* Cancer Res., 1996. **56**: p. 1189-1193.
9. Pizer, E., et al., *Inhibition of fatty acid synthesis induces programmed cell death in human breast cancer cells.* Cancer Res., 1996. **56**: p. 2745-2747.

10. Kridel, S., et al., *Orlistat is a novel inhibitor of fatty acid synthase with antitumor activity.* Cancer Res., 2004. **64**: p. 2070-2075.

11. Hinds, P., et al., *Function of a human cyclin gene as an oncogene.* PNAS, 1994. **91**: p. 709-713.

12. Petty, W., et al., *Epidermal growth factor receptor tyrosine kinase inhibition represses cyclin D1 in aerodigestive tract cancers.* Clin. Canc. Res., 2004. **10**: p. 7547-7554.

13. Martel, P., et al., *S14 protein in breast cancer cells: direct evidence for regulation by SREBP-1c, superinduction with progestin, and implication in cell growth.* submitted, 2005.

14. Kinlaw, W.B., N.C. Ling, and J.H. Oppenheimer, *Identification of rat S14 protein and comparison of its regulation with that of mRNA S14 employing synthetic peptide antisera.* J. Biol. Chem., 1989. **264**: p. 19779-19783.

15. Jensen, V., et al., *The prognostic value of oncogenic antigen 519 (OA-519) expression and proliferative activity detected by antibody MIB-1 in node-negative breast cancer.* J Pathol, 1995. **176**: p. 343-352.

16. Milgraum, L., et al., *Enzymes of the fatty acid synthesis pathway are highly expressed in in situ breast carcinoma.* Clin. Canc. Res., 1997. **3**: p. 2115-2120.

17. Menard, S., et al., *Biologic and therapeutic role of Her2 in cancer.* Oncogene, 2003. **22**: p. 6570-6578.

18. Schuuring, E., et al., *Amplification of genes within the chromosome 11q13 region is indicative of poor prognosis in patients with operable breast cancer.* Cancer Res., 1992. **52**: p. 5229-5234.

19. Champeme, M., et al., *11q13 amplification in local recurrence of human primary breast cancer.* Genes, Chromosomes, and Cancer, 1995. **12**: p. 128-133.

20. Alo, P., et al., *Expression of fatty acid synthase (FAS) as a predictor of recurrence in stage I breast carcinoma patients.* Cancer, 1995. **77**: p. 474-482.

21. Sanchez-Rodriguez, J., et al., *The spot 14 protein inhibits growth and induces differentiation and cell death of human MCF-7 breast cancer cells.* Biochem. J., 2005.

22. Heemers, H., et al., *Progestins and androgens increase expression of spot 14 in T47-D breast tumor cells.* BBRC, 2000. **269**: p. 209-212.

23. Jumar-Sinha, C., et al., *Transcriptome analysis of Her2 reveals a molecular connection to fatty acid synthesis.* Cancer Res., 2003. **63**: p. 132-139.

24. Moncur, J., et al., *Assignment of the human "spot 14' gene to 11q13.5 by fluorescence in situ hybridization.* Cytogen. Cell Genet., 1997. **78**: p. 131-132.

25. Dickson, C., et al., *Amplification of chromosome band 11q13 and a role for cyclin D1 in human breast cancer.* Cancer Letters, 1995. **90**: p. 43-50.

26. Gillet, C., et al., *Amplification and overexpression of cyclin D1 in breast cancer detected by immunohistochemical staining.* Cancer Res., 1994. **54**: p. 1812-1817.

27. Al-Kuraya, K., et al., *Prognostic relevance of gene amplifications and coamplifications in breast cancer.* Cancer Research, 2004. **64**: p. 8534-8540.

28. Courjal, F., et al., *Mapping of DNA amplifications at 15 chromosomal localizations in 1875 breast tumors: definition of phenotypic groups.* Cancer Res., 1997. **57**: p. 4360-4365.

29. Michalides, R., et al., *A clincopathological study on overexpression of cyclin D1 and of p53 in a series of 248 patients with operable breast cancer.* British J. Cancer, 1996. **73**: p. 728-734.

30. Gillett, C., et al., *Cyclin D1 and prognosis in human breast cancer.* Int. J. Cancer, 1996. **69**: p. 92-99.

31. Seshadri, R., et al., *Cyclin D1 amplification is not associated with reduced overall survival in primary breast cancer but may predict early relapse in patients with features of good prognosis.* Clin. Cancer Res., 1996. **2**: p. 1177-1844.

32. Chlebowski, R., et al., *Dietary fat reduction in postmenopausal women with primary breast cancer: Phase III Women's Interventioon Nutrition Study (WINS).* Proc. Am. Soc. Clin. Oncol., 2005. **23:3s**.

33. Weiss, L., et al., *Fatty-Acid Biosynthesis in Man, a Pathway of Minor Importance.* J Biol Chem, 1986. **367**: p. 905-912.

34. Perou, C., et al., *Distinctive gene expression patterns in human mammary epithelial cells and breast cancers.* PNAS, 1999. **96**: p. 9212-9217.

35. Desai, K., et al., *Initiating oncogenic event determines gene-expression patterns of human breast cancer models.* PNAS, 2002. **99**: p. 6967-6972.

Tables

	DCIS	Node Negative	Node Positive
Number of cases	43	34	54
Age			
Median	56	54	51
Range	31-78	41-86	27-80
% less than 50	33%	38%	46%
% 50-69	56%	56%	33%
% 70 or older	12%	6%	20%
Tumor Size			
Mean	18 mm	17 mm	36 mm
Range	2-78 mm	2-50 mm	8-100 mm
% T1		74%	30%
%T2		26%	52%
%T3			19%
Histology			
Ductal	100%	79%	83%
Lobular		12%	15%
Medullary		6%	0%
Colloid		3%	2%
Grade (Ductal Cancers Only)			
1	12%	46%	13%
2	61%	31%	42%
3	27%	23%	44%
Number of Positive Nodes			
1-3			44%
4-9			33%
10 or more			22%
Median			4
% Estrogen Receptor Positive		82%	78%
% Progesterone Receptor Positive		76%	69%
% Her-2 3+ by immunohistochemistry		26%	31%
% Treated with Mastectomy	44%	26%	70%
% Treated with Chemotherapy		38%	81%
% Treated with Hormonal Therapy	7%	59%	61%

Table I: Summary of Patient Characteristics

Tissue (n)	S14 staining (%)	FAS staining (%)
DCIS (44)		
detectable	97	97
maximal	68	97
Invasive breast cancer (88)		
detectable	99	99
maximal	76	97
Normal mammary (20)		
detectable	100	100
maximal	60	70

Table II: Frequency of S14 and FAS expression in primary breast cancers. The detectable category for S14 or FAS refers to an immunohistochemical score of 1 or 2; the maximal category corresponds to a score of 2. The normal mammary gland group included samples from 10 pre- and 10 post-menopausal women: data were pooled because there was no significant difference in staining intensities between them.

Figure Legends

Figure 1: Immunohistochemistry of S14 and FAS in lactating mammary gland. Resting mammary gland stained for S14 exhibits expression in adipocytes of the mammary fat pad, while epithelia of the rudimentary duct show little or no staining in this example (**Panel A**). Strong epithelial cell immunostaining for S14 is seen in the lobuloalveolar units of the lactating mammary gland (**Panel B**). The signal is both nuclear and cytoplasmic. Immunohistochemical analysis of lactating mammary gland using the anti-FAS antibody demonstrated strong epithelial expression of the enzyme in cytoplasm (**Panel C**).

Figure 2: Immunohistochemistry of S14 and FAS in breast tumors. Examples of DCIS (**left column**) and an invasive ductal carcinoma (**right column**) are shown. The **upper panels** are negative controls processed without primary antibody and stained with hematoxylin. S14 showed primarily nuclear staining (**middle panels**) that was of maximal intensity in 68% of DCIS and 97% of invasive cases. FAS immunoreactivity (**lower panels**) was cytoplasmic. Maximal staining, as exemplified in the cases shown, was found in 76% and 97% of DCIS and invasive tumors, respectively.

Figure 3: Relationship of S14 content to tumor grade and size. The frequency of strong staining in normal mammary tissue is indicated by the blue bar. *Upper panel-* Analysis of S14 staining in DCIS (n=44) as a function of histological grade; *Middle panel-* Pooled data from invasive breast cancers without (n=34) or with (n=54) lymph node metastases at the time of

diagnosis, stratified by tumor grade. *Lower panel-* Pooled data from invasive cases (n=88) as a function of tumor size.

Fig. 4: Disease-free survival of patients after treatment of invasive breast cancer as a function of S14 expression in the primary tumor. Kaplan-Meier analysis of patients with and without positive lymph nodes at initial surgery is shown. Patients with an immunohistochemical score of 0 or 1+ (n=21) are represented by the solid line, and those with a 2+ S14 score by the dotted line (n=67). The difference between the two plots was statistically significant (p=0.015).

Fig. 5: Disease free survival in patients with invasive breast cancer as a function of S14 scores and the presence or absence of lymph node metastases at initial surgery. The same patients represented in Figure 4 are analyzed. Patients with negative lymph nodes and submaximal S14 scores (n=11) or positive lymph nodes and low S14 scores (n=10) are represented by the top tracings, which are superimposed because there were no recurrences in those groups. Among patients with negative lymph nodes and a high S14 scores (n=23), one recurred after ~ 2000 days follow-up (dashed line). Among the patients with nodal metastasis and strong S14 staining (n=44), there were 14 recurrences (log rank $p<0.0001$).

Figures

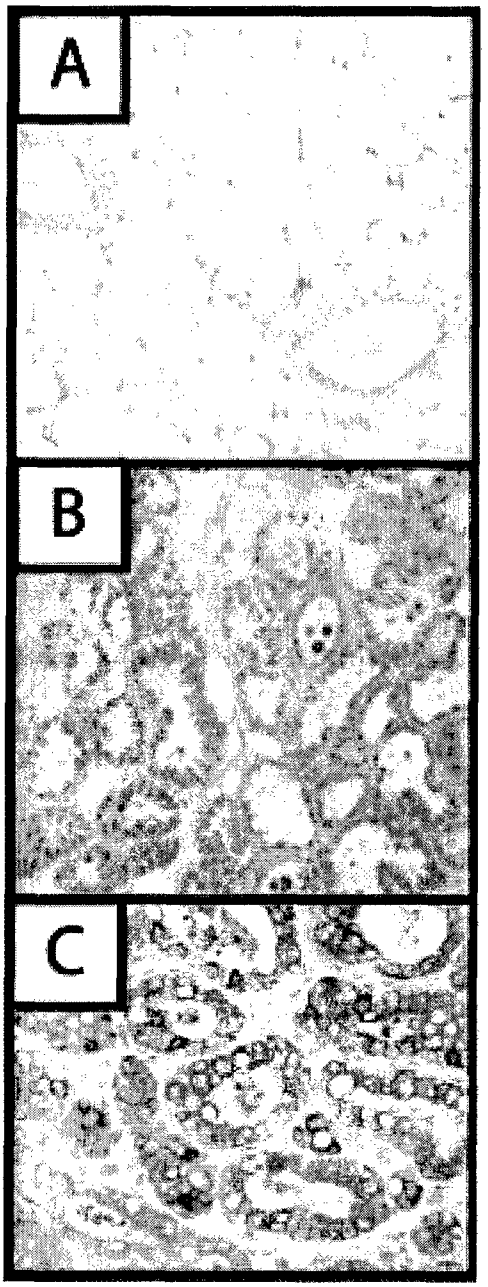

Fig. 1

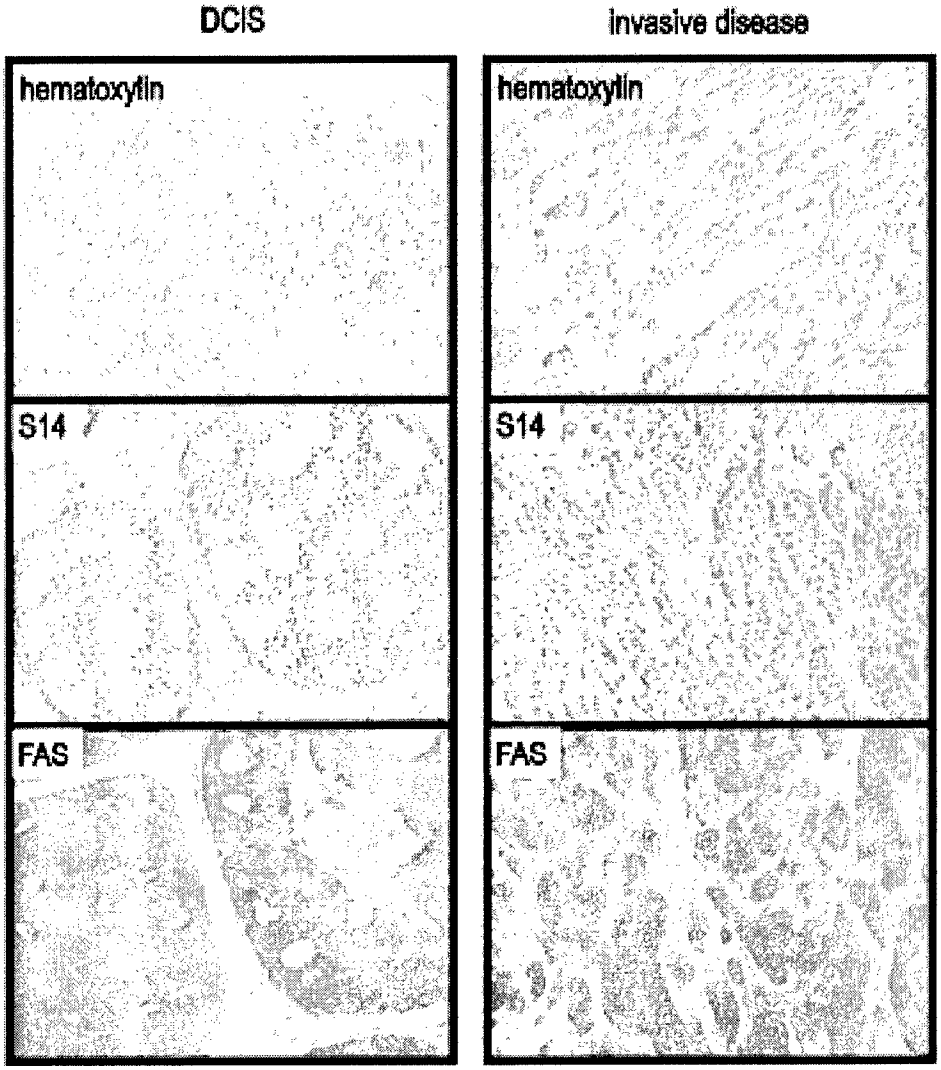
DCIS
invasive disease
hematoxylin
hematoxylin
S14
S14
FAS
FAS

Fig. 2

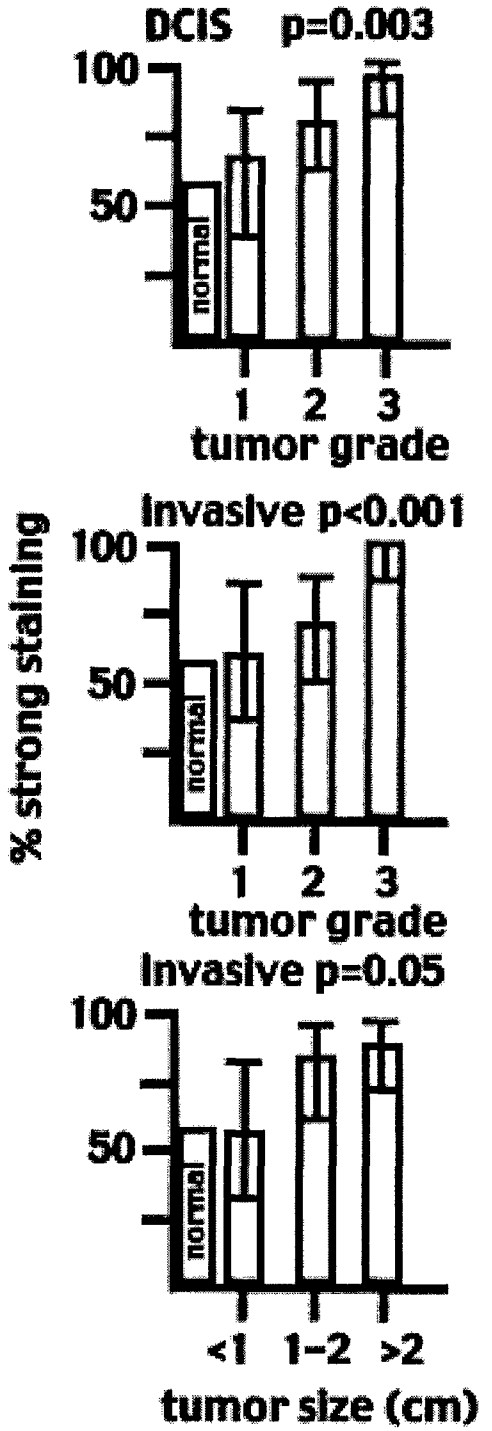
DCIS p=0.003
100
50
normal
1 2 3
tumor grade
Invasive p<0.001
% strong staining
100
50
normal
1 2 3
tumor grade
Invasive p=0.05
100
50
normal
<1 1-2 >2
tumor size (cm)

Fig. 3

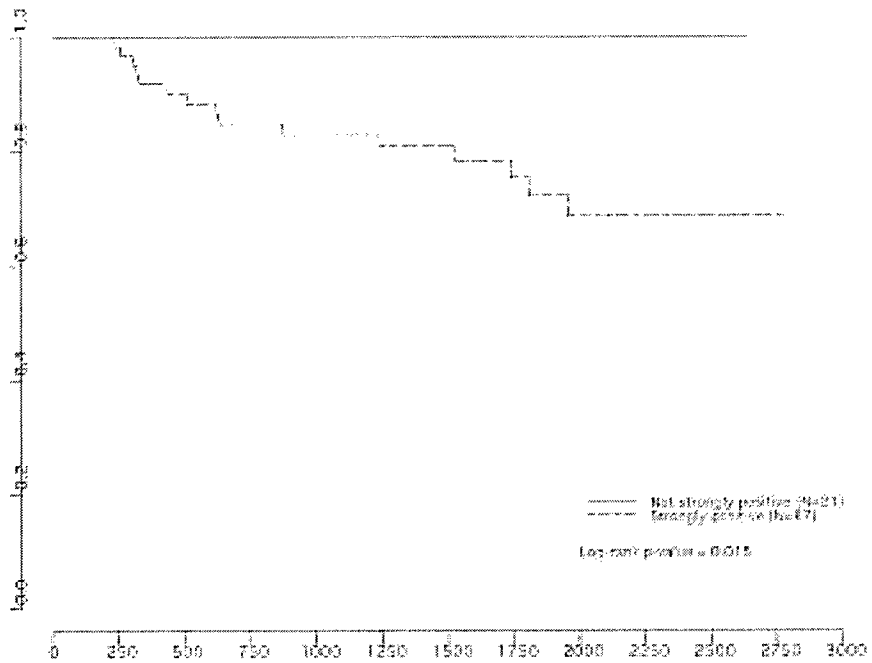
1.0
0.8
0.6
0.4
0.2
0.0
0
250
500
750
1000
1250
1500
1750
2000
2250
2500
2750
3000

Fig. 4

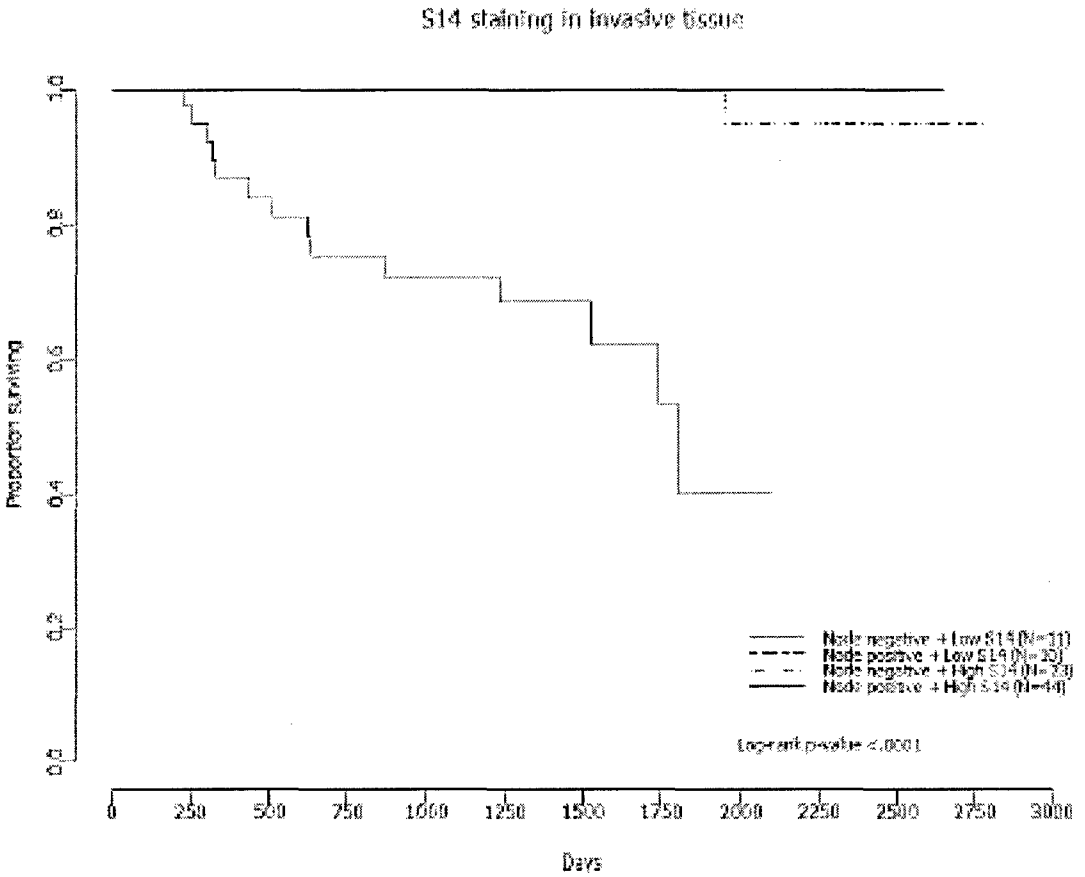
S14 staining in invasive tissue
Proportion surviving
0.0
0.2
0.4
0.6
0.8
1.0
0
250
500
750
1000
1250
1500
1750
2000
2250
2500
2750
3000
Days
Node negative + Low S14 (N=11)
Node positive + Low S14 (N=30)
Node negative + High S14 (N=23)
Node positive + High S14 (N=44)
Log-rank p-value <.0001

Fig. 5

KINLAW Appendix item #3

METABOLIC REGULATOR AND THERAPEUTIC TARGET S14 IS UBIQUITOUS IN BREAST CANCER AT ALL STAGES AND INCREASES WITH TUMOR GRADE. IMMUNOHISTOCHEMICAL ANALYSIS OF 132 CASES AND COMPARISON WITH FATTY ACID SYNTHASE.

William B. Kinlaw[1,3], Jennifer Gibson Chambers[3], Bernard Cole[3], Gary N. Schwartz[1,3], Wendy A. Wells[1,3] Departments of Medicine[1,3], Pathology[2],and The Norris Cotton Cancer Center[3], Dartmouth Medical School, Lebanon, NH 03756.

Corresponding author- William.Kinalw@Hitchcock.org

Most breast cancers are "lipogenic", defined by high fatty acid synthase (FAS) content, and require *de novo* fatty acid synthesis for growth and survival. S14 is a glucose- and hormonally-inducible nuclear protein that activates genes required for fatty acid synthesis, including FAS, and S14 knockdown causes breast cancer cell apoptosis. The S14 locus at 11q13 is amplified in ~13% of breast cancers, but the prevalence of S14 expression and its clinical correlates are unknown. We generated an anti-S14 monoclonal antibody to immunohistochemically analyze 132 breast cancers diagnosed at Dartmouth 1996-98 (44 non-invasive (DCIS); 34 locally invasive, node negative; 54 invasive, node positive) and 20 cases of normal mammary tissue. S14 and FAS expression was graded 0, 1, or 2+. S14 and FAS were detectable in ≥97% of cancers and normal controls. Strong S14 signals occurred in 89% of DCIS and 76 % of invasive disease (p=NS), and did not differ between node (-) and (+) cases. Strong FAS staining was observed in ≥97 % of DCIS and invasive cases, confirming published data. S14 or FAS staining alone were not related to tumor stage, whereas a 2+ signal for both was more frequent in DCIS than invasive cases (79 vs. 51%, p<0.001). Strong S14 staining was related to tumor size (<1.0 cm 58%, 1.0-2.0 cm 80%, > 2.0 cm 83%; p=0.05). The S14 signal was also related to tumor grade in both DCIS and invasive cases, whereas this was not the case for FAS. Strong S14 reactivity in grade 1/2/3 DCIS was 62/76/97% (p=0.003) and 61/70/100% in invasive cases (p<0.001). Normal control mammary gland showed strong S14 signals in 60% of cases, similar to low grade and small cancers. Progestin induces S14 in breast cancer cells, but expression did not vary with sex steroid receptor status in tumors. Interestingly, normal mammary epithelium adjacent to DCIS showed more S14 than that near invasive tumors (85 vs. 47% 2+ signal, p<0.001). We conclude that 1) S14 is detectable in >98% of breast cancers, and highly expressed in 76% of invasive cases; 2) Mechanisms other than gene amplification must underlie its abundant expression in most tumors; 3) Rather than being acquired during progression, strong S14 expression occurs in early stage disease; 4) Intensity of the S14, but not FAS, signal increases with histological grade in both DCIS and invasive disease. We speculate that reduced S14 in normal epithelia adjacent to invasive tumors, as opposed to DCIS, reflects local deficiency of a nutrient such as glucose. S14 could be a useful metbolism-related marker for high-grade breast cancer, and its presence in essentially every case enhances its clinical potential as a therapeutic target.